

UK Inflation Dynamics since the Thirteenth Century

Online Supplement

James M. Nason and Gregor W. Smith[†]

17 May 2023

[†]Nason: Centre for Applied Macroeconomic Analysis, Australian National University, and Virginia Center for Economic Policy, University of Virginia; *jmnason87@gmail.com*.

Smith: Department of Economics, Queen's University, Canada; *gregor.smith@queensu.ca*.

Table of Contents

	Page
Appendix A: Alternative Price Indexes	1
Appendix B: Alternative Models	6
Appendix B.1: Measurement Error with AR(1)	6
Appendix B.2: Alternative Models of Measurement Error	6
Appendix B.3: The TVP-SV-AR(n) minus Measurement Error	19
Appendix B.4: The Horseshoe Prior	27
Appendix C: A MH in Gibbs MCMC Sampler	37
Appendix D: The Formula for Inflation Predictability	47
Appendix E: The Formula for Price-Level Instability	49
References	55

Appendix A: Alternative Price Indexes

An alternative to the Clark index is the Bank of England CPI series assembled by Thomas and Dimsdale (2016). Prior to 1661 it uses a slightly different version of the Clark index that applies to the poorest workers and excludes services. Thomas and Dimsdale adopt the Schumpeter-Gilboy index from Mitchell (1988) for 1661–1750, the series from Crafts and Mills (1991) for 1750–1770, the series from Feinstein (1998) for 1770–1882, the series from Feinstein (1991) for 1882–1914, the series from the ONS (O’Donoghue, Goulding, and Allen, 2004) for 1914–1949, and the CPI (ONS) for 1949–2016. There are 807 observations in this series up to 2016.

Allen (2001) constructed a city-level CPI for London and for a number of other European cities. These are Laspeyres indexes using what he describes as a ‘pre-modern basket’ (given in his table 3). The basket differs across cities depending on the local food and fuel sources. As is usual with early price indexes, the data sources tend to be institutions such as hospitals or schools but one of Allen’s many contributions is to use retail bread prices rather than grain prices. For London the Allen series spans 1264–1913 or 649 observations. Allen notes his London index closely tracks that of Feinstein (1998) when they overlap. There does not appear to be a London-level CPI after 1913 to which to splice this series.

The Allen and Clark series differ in several respects: (i) Clark uses data from throughout England and later the UK while Allen applies to London; (ii) Allen omits lodging (though for the early period this was a relatively small share of expenditure), manufactures such as tools, and services; (iii) Clark’s weights change over time; (iv) both series use bread rather than grain but they estimate the retail bread price in different ways.

Figure A1 shows the logs of the Clark series (in blue), the Bank of England series (in red, dashed), and the Allen series (in green, dotted) for four periods each of roughly two centuries: 1209–1399; 1400–1599; 1600–1799; and 1800–2019. The Bank of England series is rescaled so that 2010 = 100 as for the Clark series. The Allen series is rescaled so that it is equal to the Clark series when it ends in 1913. The Bank of England series and the Allen series are more volatile than the Clark series, perhaps because of the categories of consumption spending that they omit.

Cogley, Sargent, and Surico (2015) use a price index found in Mitchell (1988). He

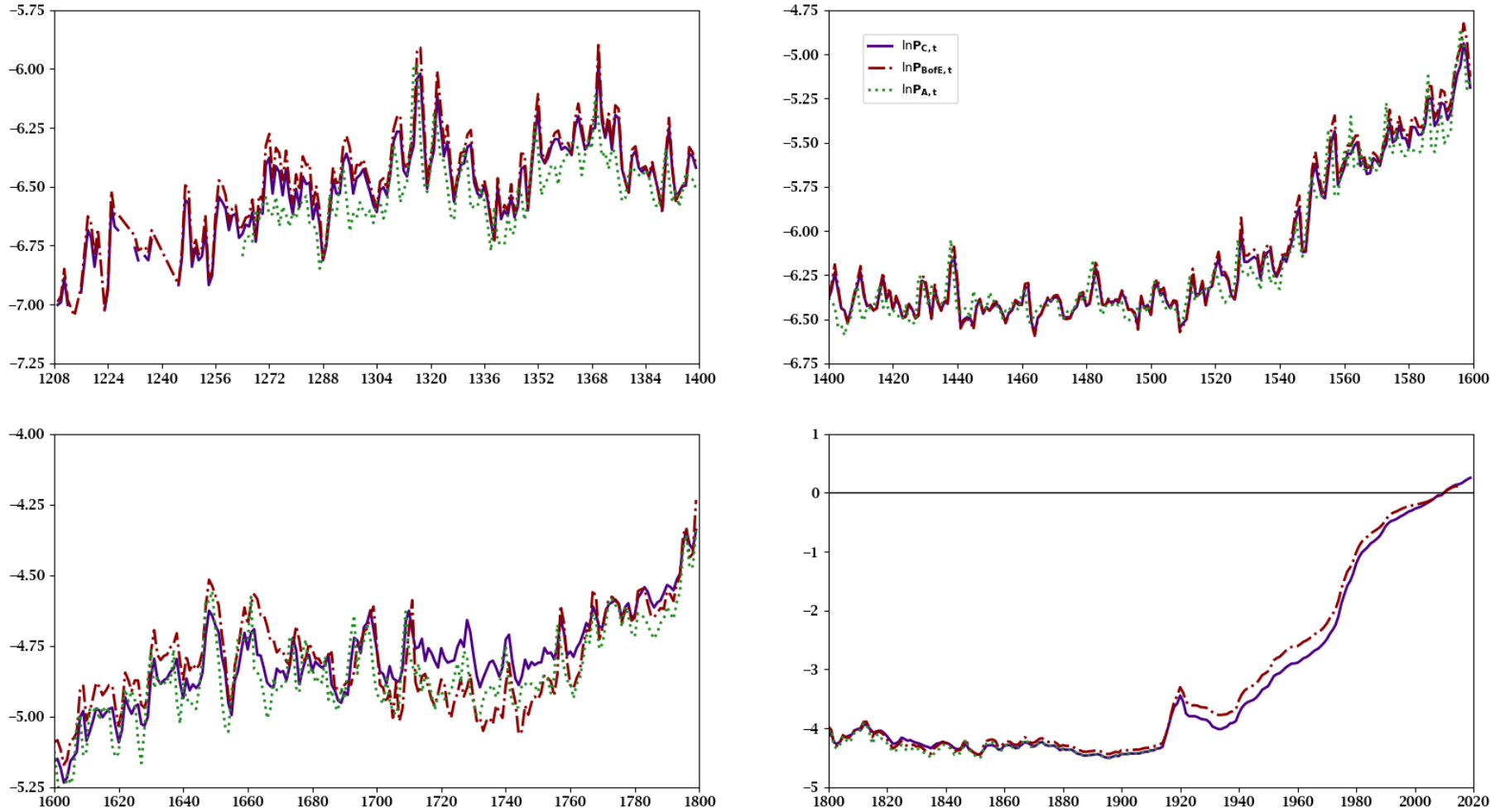
spliced together indexes from Lindert and Williamson for 1781–1846 and from Bowley for 1846–1914. We rescale the Mitchell series so that it is equal to the Clark series in 1913. Figure A2 then graphs the log price level from Clark (in blue, as above) and Mitchell (in red, dashed) for 1781–1947. Two obvious differences are in the 1946–1947 inflation rates and particularly in the greater volatility of the Lindert-Williamson and Bowley inflation rate series compared to the Clark series. We claim no expertise in deciding which is the best index, but simply note that the greater volatility of the early Mitchell series seems due to the Lindert-Williamson data. This volatility is not evident in more recently constructed series such as those of Clark or the Bank of England.

There is one further source of price data that informs our design. *The Statist*, a competitor of *The Economist*, published a commodity price index from 1848 to 1950. This series is known as the Sauerbeck-Statist Index, named for its founder Augustus Sauerbeck. It was annually reported in the *Journal of the Royal Statistical Society (A)* and we collected the annual averages from that periodical (1950) 114(3) 408–422.

The Sauerbeck-Statist index is very similar to the Warren-Pearson data (extended by Hanes) for the US studied by Cogley and Sargent (2015). That too is an arithmetic commodity price index. But of course a difference is that they did not have a broader retail price index for early periods, and so used the relationship when the two series overlapped to inform a prior over measurement error in the earlier commodity price index and so draw inference about the unobserved retail price index. In contrast, for the UK there is a direct source—though no doubt error-laden—for each period.

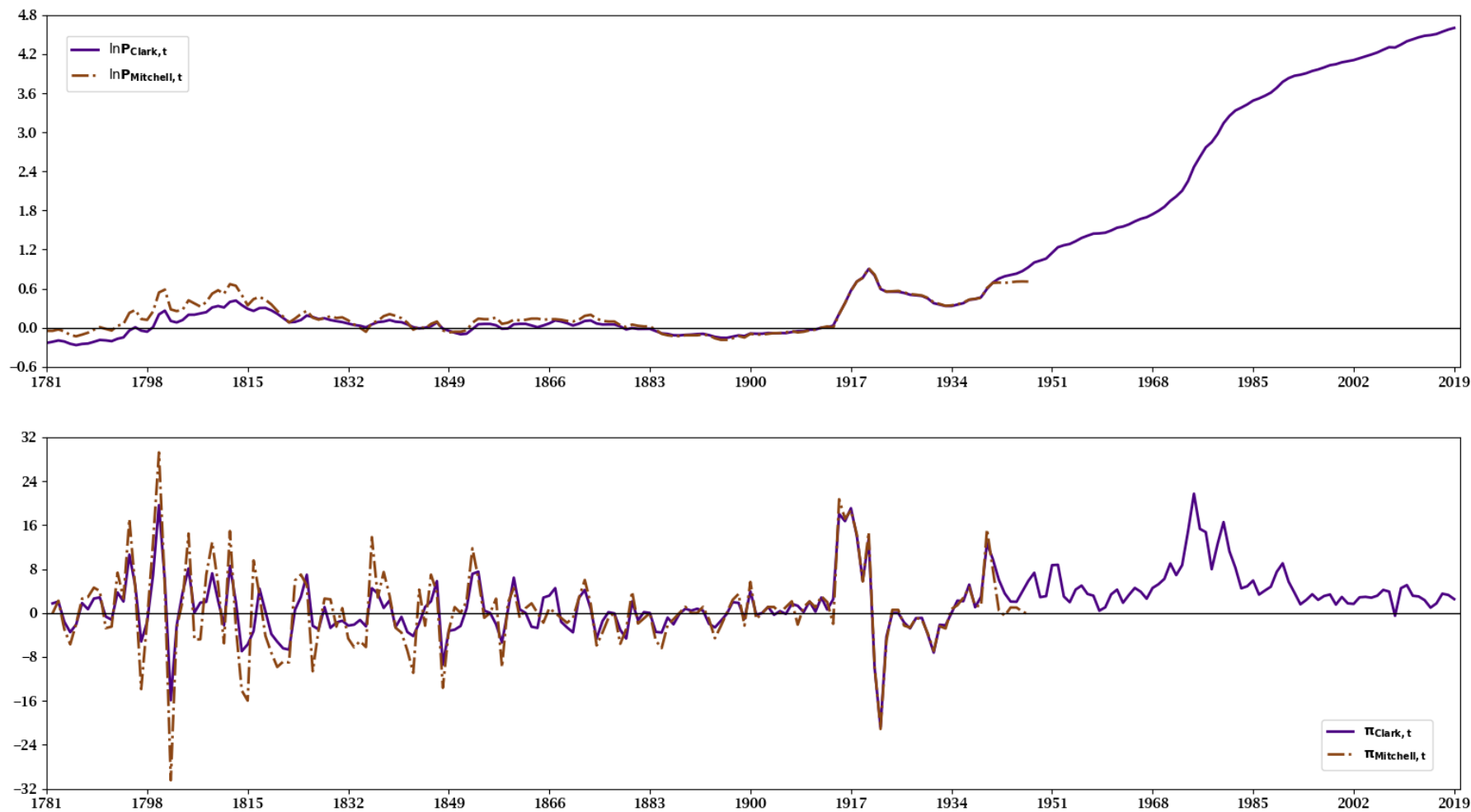
Figure A3 shows the log price index and inflation rate for the Clark data used in the paper (in black) and for Sauerbeck-Statist data (in blue). Notice that the commodity price inflation rate is more volatile than the retail price inflation rate. However, Figure A3 shows that this ratio of variances does not change much over time. At least from this comparison, then, there is not great measurement error in the Feinstein data (1870–1914) data relative to that in the next span (1915–1946) when the official cost-of-living index was collected. This fact motivates our prior that β_2 and β_3 are fractions that scale down measurement error relative to that in the early centuries of the $p_{uk,t}$ series.

Figure A1: The Clark-, Bank of England-, and Allen-UK Price Levels on Several Subsamples



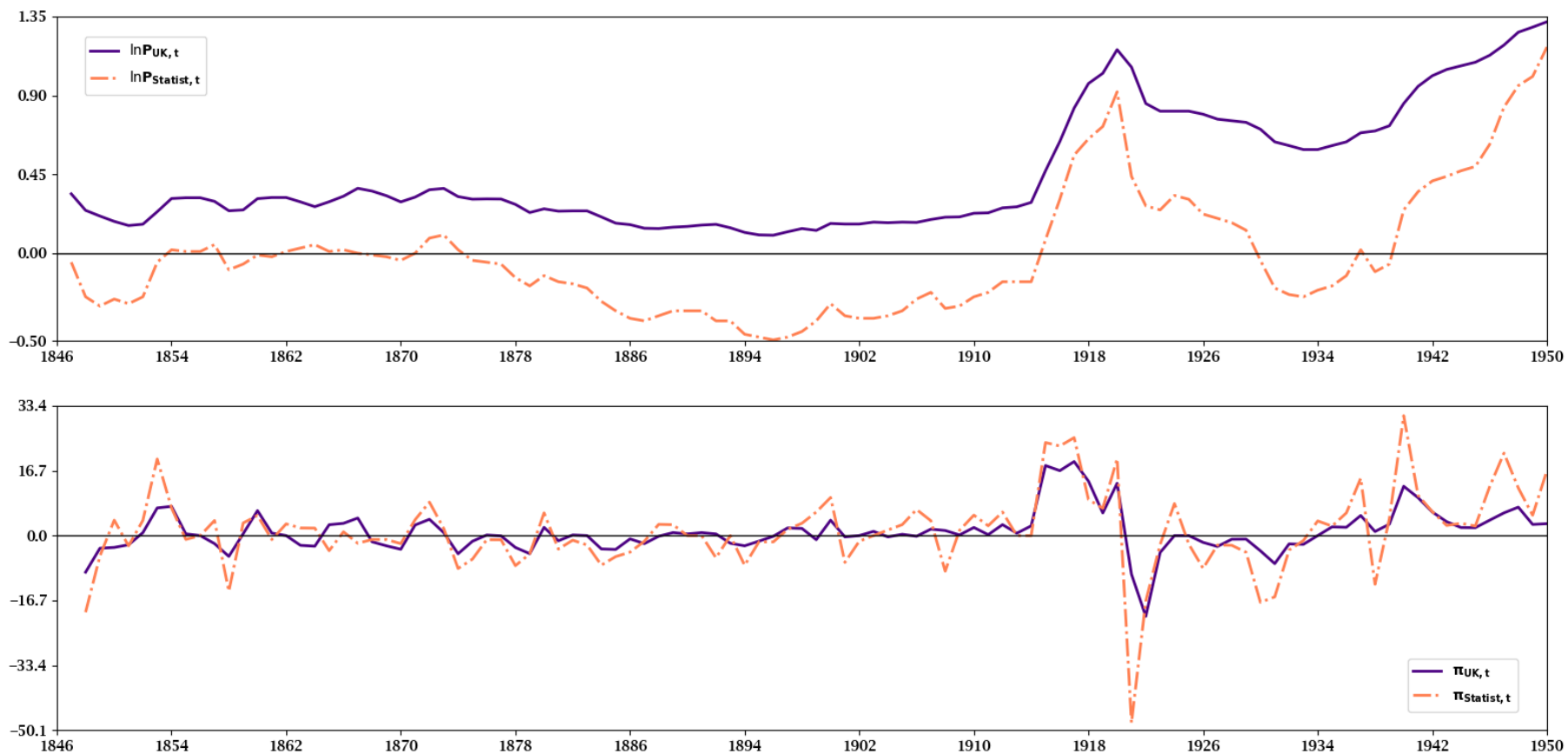
Notes: The panels depict the natural logs of the Clark-, Bank of England-, and Allen-UK price levels, $p_t = \ln(P_t/100)$. The top right, top left, bottom left, and bottom right panels plots these price levels from 1209 to 1399, 1400 to 1599, 1600 to 1799, and 1800 to 2019. The samples of the Clark-, Bank of England-, and Allen-UK price data run from 1208 to 2019, 1208 to 2016, and 1263 to 1913, respectively. The Bank of England price level is rescaled for it to equal 100 in 2010 as is the Clark series. The Allen series is rescaled to force its last observation in 1913 to equal the Clark series at that date.

Figure A2: The Clark- and Mitchell UK Price Level and Inflation Rates, 1781–2019



Notes: The top panel contains the natural log of the price level of the Clark- and Mitchell-UK price series while the bottom panel plots the inflation rates. The Mitchell-UK price sample runs from 1781 to 1947. The Clark UK-price sample ends in 2019.

Figure A3: UK and Statist Price Level and Inflation, 1847–1950



Notes: The top panel displays the log level of the UK long annual price index as the solid (indigo) line and dot-dashed (coral) line, which is the Sauerbeck-Statist commodity price index, from 1847 to 1950. The associated inflation rates appear in the bottom panel from 1848 to 1950.

Appendix B: Alternative Models of Measurement Error

We considered other models of measurement error that start with equation (1), as noted in section 4. This section summarizes these models of measurement error.

Appendix B.1. Measurement Error with AR(1) Persistence

First, attempts were made to tie measurement error to the log price level, $p_{uk,t}$, instead of inflation, $\pi_{uk,t}$. In these cases, the additive measurement error process was assumed to be a AR(1) across the spans $\tau = 1, 2$, and 3 , but $\rho_4 = 0$. Draws from the posterior of these models often gave estimates of the AR1 coefficient that were greater than one. Since these models of measurement error are non-stationary, we decided not to pursue them.

Second, we tried to parametrize the additive measurement error on $\pi_{uk,t}$ as a AR(1) process, where the AR1 parameter ρ_τ is constant within the spans. Priors on ρ_τ are drawn from a mean zero normal distribution with a variance of 0.5 that is truncated to guarantee $\rho_\tau \in (-1, 1)$ for $\tau = 1, 2$, and 3 and $\rho_4 = 0$. The result is prior 90% coverage intervals of ± 0.83 . Posterior densities of ρ_1, ρ_2 , and ρ_3 were found to have medians (with 5%–95% IQRs) equal to 0.09 (-0.06, 0.23), 0.24 (-0.13, 0.58), and 0.19 (-0.23, 0.61). Thus there is considerable uncertainty in the posterior about these parameters, which increases with τ , yielding 90% Bayesian credible sets for ρ_1, ρ_2 , and ρ_3 that cover zero. Furthermore, posteriors of β_2, β_3 , and σ_u^2 , were close to those reported in the paper and in Figure 3.

Third, a measurement error model with AR(1) persistence was estimated inspired by Cogley and Sargent (2015), Cogley, Sargent, and Surico (2015) and Amir-Ahmadi, Matthes, and Wang (2016). Along with constant persistence within each span, the variance, $\sigma_{\tau,u}^2$, of the AR(1) is fixed on an inverse-gamma (\mathcal{IG}) prior for $\tau = 1, 2$, and 3 while $\sigma_{4,u}^2 = 0$. Table B2 lists these priors, which are also used for the alternative model of iid measurement error discussed in the next section. For the AR(1) model of measurement error at hand, we obtain no evidence that ρ_1, ρ_2 , and ρ_3 differ from zero.

Appendix B.2. An Alternative Model of iid Measurement Error

We also estimated an alternative measurement error model in which $m_t = \sigma_{\tau,u} u_t$ replaces equation (2). This model of iid measurement error assumes, as do Cogley and Sargent (2015), Cogley, Sargent, and Surico (2015), and Amir-Ahmadi, Matthes, and Wang

(2016), that the variances, $\sigma_{\tau,u}^2$, are unrestricted, other than being strictly positive, for $\tau = 1, 2$, and 3 . However, our much longer first span, from 1251 to 1869, and the availability of improved 19th century data since Mitchell (1988) that are associated with the work of Feinstein, Clark, Crafts and Mills, and others, motivate our choice of priors that have the variance of measurement error decreasing over the spans.

Table B2 describes \mathcal{IG} priors for $\sigma_{1,u}^2$, $\sigma_{2,u}^2$, and $\sigma_{3,u}^2$ that reflect our belief about the declining volatility of measurement error across the 1251-1869, 1870-1914, and 1915-1946 spans. The \mathcal{IG} priors are constructed to produce these restrictions, according to our choices of the scale and shape parameters, θ_1 and θ_2 . We set $\theta_1 = \psi_{1,\tau}T_\tau$, where $\psi_{1,\tau}$ increases with τ , but $\psi_{1,4}$ is zero, and T_τ is the length of the span τ . Since the shape parameter of an \mathcal{IG} distribution is a function of the variance, we equate θ_2 to a fraction, $\psi_{2,\tau}$, of the prior variance of $\sigma_{\tau,u}^2$, σ_{PR}^2 . Our prior reduces $\psi_{2,\tau}$ as τ increases to lower the variance of $\sigma_{\tau,u}^2$ at the same time. As the notes to Table B2 discuss, this parametrization shifts the median and 5%–95% IQRs of $\sigma_{2,u}^2$ to the left of $\sigma_{1,u}^2$ and $\sigma_{3,u}^2$ to the left of $\sigma_{2,u}^2$.

The same MH in Gibbs MCMC sampler is applied to the alternative iid measurement error model of equation (1), $m_t = \sigma_{\tau,u}u_t$, and equations (3)-(5) as to the baseline measurement error model of equations (1)-(5) in the paper; see Appendix C below for details. Table B3 presents ln MDDs and WAICs for the alternative iid model of measurement error. For comparison, we also include the same statistics found in Table 4 for the baseline measurement error model. The ln MDDs indicate (at least) substantial support for a lag length of $n = 3$ as shown in the bottom half of Table B3. The WAICs lead to the same conclusion. Hence both models of measurement error yield the same inference for the lag length of the TVP-SV-AR(n) of π_t . Nevertheless, the evidence is decisive, according to the ln MDDs at $n = 3$, that the data prefer the baseline model of iid measurement error as described by equations (1)-(5) in the paper.

Information about the posteriors of $\sigma_{1,u}^2$, $\sigma_{2,u}^2$, and $\sigma_{3,u}^2$ are presented in Table B3 for $n = 1, \dots, 6$. Three features stand out in the table. First, the medians of the posteriors of these variances increase from the first (1251–1869) span to the second (1870–1914) span and then again to the third (1915-1946) span across all lag lengths. Second, at all lag lengths the 90% Bayesian credible sets of $\sigma_{1,u}^2$ are to the left of the 90% Bayesian credible

sets of $\sigma_{2,u}^2$. Third, as n increases, the medians of the posteriors of $\sigma_{1,u}^2$, $\sigma_{2,u}^2$, and $\sigma_{3,u}^2$ also increase along with the corresponding 90% Bayesian credible sets shifting to the right.

Table B4 summarize the posteriors of β_2 , β_3 , and σ_u^2 . The medians of the posteriors of these measurement error parameters also increase as the lag length of TVP-SV-AR(n) moves from one to six lags. At the same time, the 90% Bayesian credible sets shift to the right. However, at the medians of the posteriors $\beta_2 > \beta_3$ across all lag lengths. Finally, notice that estimates of σ_u^2 are always close to the estimates of $\sigma_{1,u}^2$ in Table B3.

Figures B1–B6, which correspond to Figures 3–8 in the text, show the posterior results for the alternative iid measurement error model. As noted in the text, economic conclusions drawn from the alternative model of measurement error are strikingly similar to the results reported in the paper. Nonetheless, there is one important finding for the alternative model of measurement error that is reminiscent of the volatility puzzle reported by Cogley, Sargent, and Surico (2015). The puzzle is more recent UK inflation data seemingly is more ridden with measurement error than are earlier data.

There is increasing volatility in the median of the posterior of the alternative iid model’s smoothed measurement error moving from span 1 to span 2 and again from span 2 to span 3, as seen in the lower right panel of Figure B1. The increasing volatility is also apparent in the 68% uncertainty bands surrounding the median of smoothed measurement error. This is the puzzle that Cogley, Sargent, and Surico (2015) find in estimates of their unobserved components (UC) model, which treats inflation as non-stationary. This shows the puzzle can arise when inflation is modeled as a non-stationary UC model or as a stationary AR(n) with TVP and SV. Mechanically, the puzzle is driven by observations, as in 1920–1922, which were preceded by high inflation at the end of World War I and followed by ten years of deflation, yielding the sawtooth pattern in inflation observed in Figure 1. By the time our MCMC sampler finds that persistence in inflation is substantial and its SV falling, it attributes at least part of this behavior to measurement error.

There are two reasons the measurement error that we find is not comparable to that in Cogley, Sargent, and Surico (2015). First, we rely on the Clark data whereas they engage the more volatile Mitchell data for the 19th century, as discussed in Appendix A. Second, our longer sample starts in 1251, but their first span begins in the late 18th century.

Table B1: Alternative Model of Measurement Error

$$\pi_{uk,t} = \pi_t + m_t,$$

$$m_t = \sigma_{\tau,u} u_t,$$

$$u_t \sim \mathcal{N}(0, 1).$$

Measurement Error	Prior	Parameters	
Scale Volatility	Distribution	θ_1	θ_2
$\sigma_{\tau,u}^2$	\mathcal{IG}	$\psi_{1,\tau} T_\tau$	$\psi_{2,\tau} \sigma_{PR}^2$

Notes: The \mathcal{IG} prior on the variance, $\sigma_{\tau,u}^2$, of measurement error, m_t , relies on τ . The shape parameter $\theta_1 = \psi_{1,\tau} T_\tau$ and scale parameter $\theta_2 = \psi_{2,\tau} \sigma_{PR}^2$. For $\tau = 1$ (1251–1869), 2 (1870–1914), 3 (1915–1946), and 4 (1947–2019), $\psi_{1,\tau} = [0.004 \ 0.060 \ 0.075 \ 0.000]'$, $T_\tau = [619 \ 45 \ 32 \ 74]'$, and $\psi_{2,\tau} = [0.85 \ 0.65 \ 0.50 \ 0.00]'$. The scale parameter is a sufficient statistic for the variance of a random variable drawn from an \mathcal{IG} distribution. This explains equating the prior variance σ_{PR}^2 to 0.21114^2 , which is the variance of UK inflation on the Bank of England data from 1209 to 1244; see Thomas and Dimsdale (2016). These parametrizations give $\sigma_{1,u}^2$, $\sigma_{2,u}^2$, and $\sigma_{3,u}^2$ prior 5th, 50th, and 95th quantiles of $[0.007, 0.017, 0.067]$, $[0.005, 0.012, 0.043]$, and $[0.004, 0.011, 0.042]$. Otherwise, see Table 3 of the paper for the priors on the covariance matrix of innovations to the TVPs, Ω_η , and initial conditions of α_0 and $\ln \xi_0^2$.

**Table B2: Evaluation of Fit of the TVP-SV-AR(n)s
with Baseline and Alternative Models of Measurement Error**

	AR(1)	AR(2)	AR(3)	AR(4)	AR(5)	AR(6)
Baseline:						
ln MDD	638.21	643.18	673.62	667.59	652.72	650.82
WAIC	-1431.95	-1457.55	-1487.87	-1483.30	-1487.75	-1465.82
Alternative:						
ln MDD	558.29	608.73	616.77	615.49	607.72	592.70
WAIC	-1336.86	-1370.68	-1398.40	-1389.88	-1383.41	-1371.86

Notes: See the notes to Table 4 of the paper.

**Table B3: Summary of the Posterior Distributions
of the Parameters of the Alternative Model of iid Measurement Error**

n	$\sigma_{1,u}^2$	$\sigma_{2,u}^2$	$\sigma_{3,u}^2$
1	0.00167 [0.00129, 0.00215]	0.00381 [0.00239, 0.00650]	0.00438 [0.00242, 0.00838]
2	0.00163 [0.00128, 0.00212]	0.00379 [0.00235, 0.00667]	0.00436 [0.00243, 0.00882]
3	0.00165 [0.00130, 0.00215]	0.00390 [0.00237, 0.00662]	0.00438 [0.00238, 0.00904]
4	0.00167 [0.00129, 0.00217]	0.00404 [0.00247, 0.00718]	0.00459 [0.00252, 0.00923]
5	0.00170 [0.00131, 0.00223]	0.00421 [0.00252, 0.00755]	0.00467 [0.00255, 0.00934]
6	0.00175 [0.00133, 0.00229]	0.00428 [0.00263, 0.00757]	0.00486 [0.00260, 0.00971]

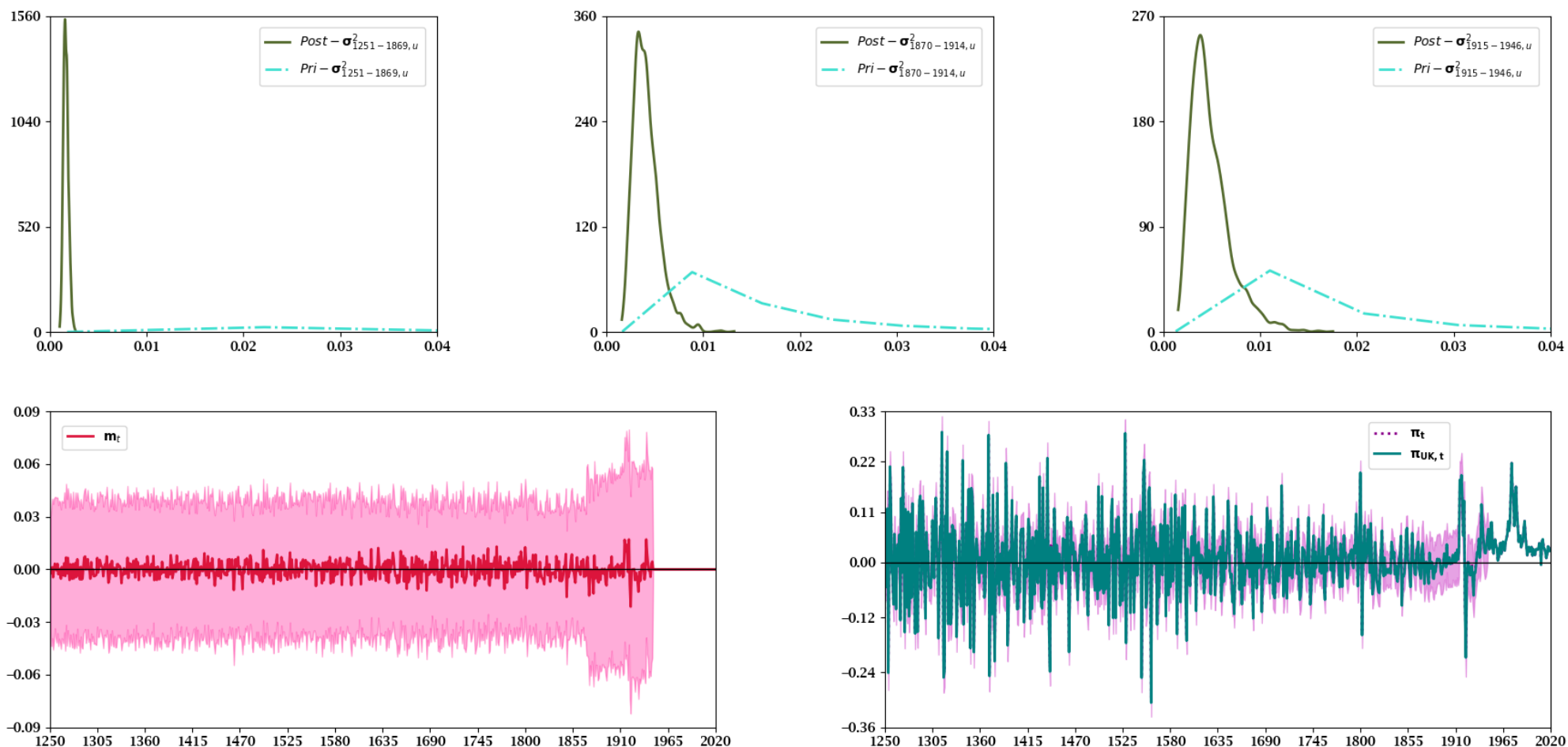
Notes: The table displays medians of posteriors of the scale volatilities, $\sigma_{\tau,u}^2$ of the alternative model of measurement error for the TVP-SV-AR(n), where $\tau = 1$ (1251–1869), 2 (1870–1914), and 3 (1915–1946) and $n = 1, \dots, 6$. Below these estimates, the brackets contain five and 95% quantiles extracted from the posterior distributions.

**Table B4: Summary of the Posterior Distributions
of the Parameters of the Baseline Model of Measurement Error**

n	β_2	β_3	σ_u^2
1	0.44397 [0.18966, 0.75997]	0.28199 [0.09809, 0.56736]	0.00164 [0.00130, 0.00210]
2	0.44707 [0.20009, 0.75827]	0.28315 [0.09548, 0.57860]	0.00161 [0.00126, 0.00208]
3	0.44188 [0.19638, 0.74622]	0.29022 [0.09389, 0.58692]	0.00163 [0.00128, 0.00208]
4	0.45117 [0.19936, 0.76018]	0.29683 [0.09696, 0.58665]	0.00165 [0.00131, 0.00213]
5	0.46425 [0.20242, 0.77210]	0.29407 [0.10279, 0.56927]	0.00168 [0.00132, 0.00217]
6	0.46626 [0.20216, 0.76205]	0.30778 [0.10459, 0.59067]	0.00172 [0.00135, 0.00224]

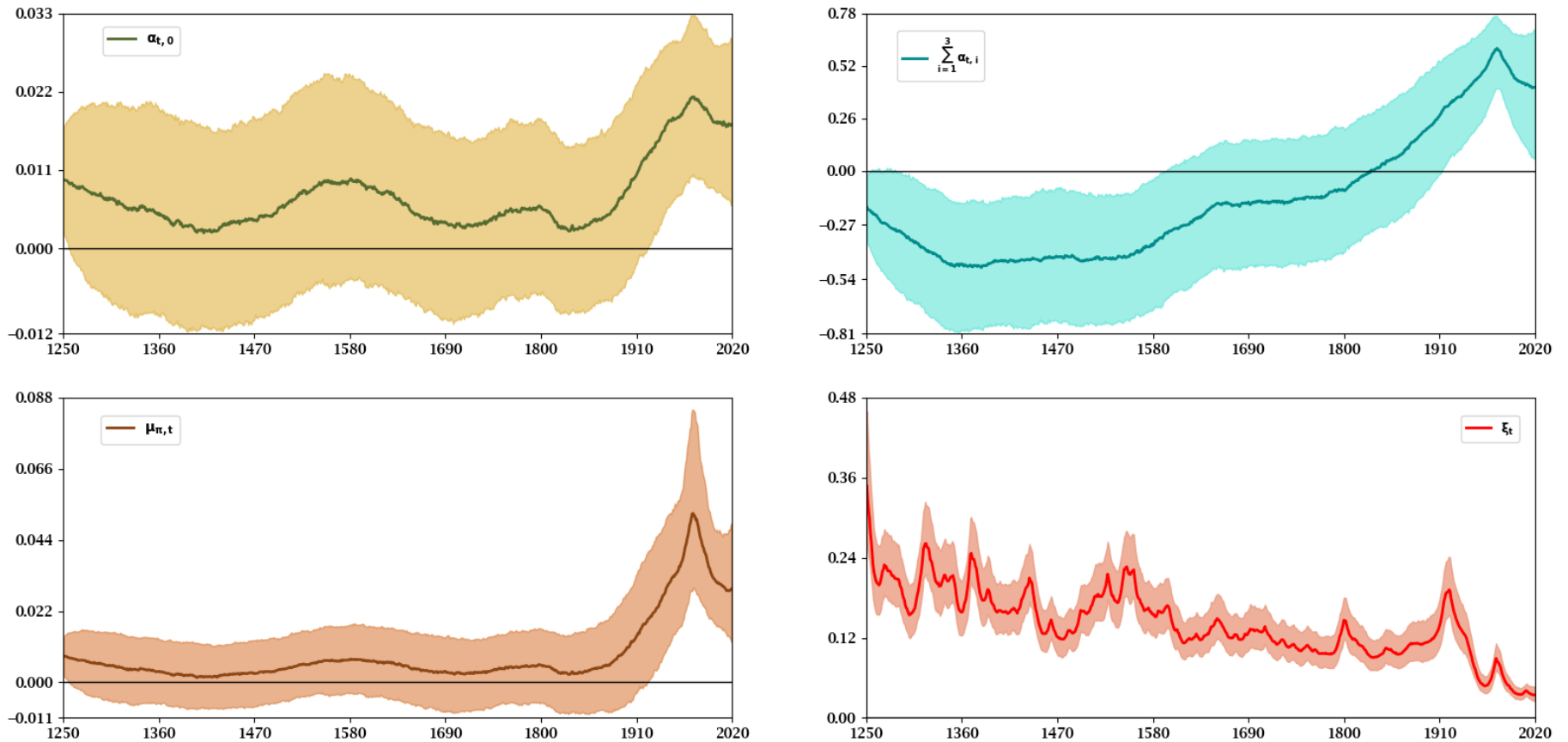
Notes: The table reports medians of the posteriors of the baseline model measurement error parameters, β_2 (1879–1914) and β_3 (1915–1946), and scale volatility, σ_u^2 , for the TVP-SV-AR(n), $n = 1, \dots, 6$. Below these estimates, the brackets contain five and 95% quantiles extracted from the posterior distributions.

Figure B1: Measurement Error Parameter Densities and Smoothed States



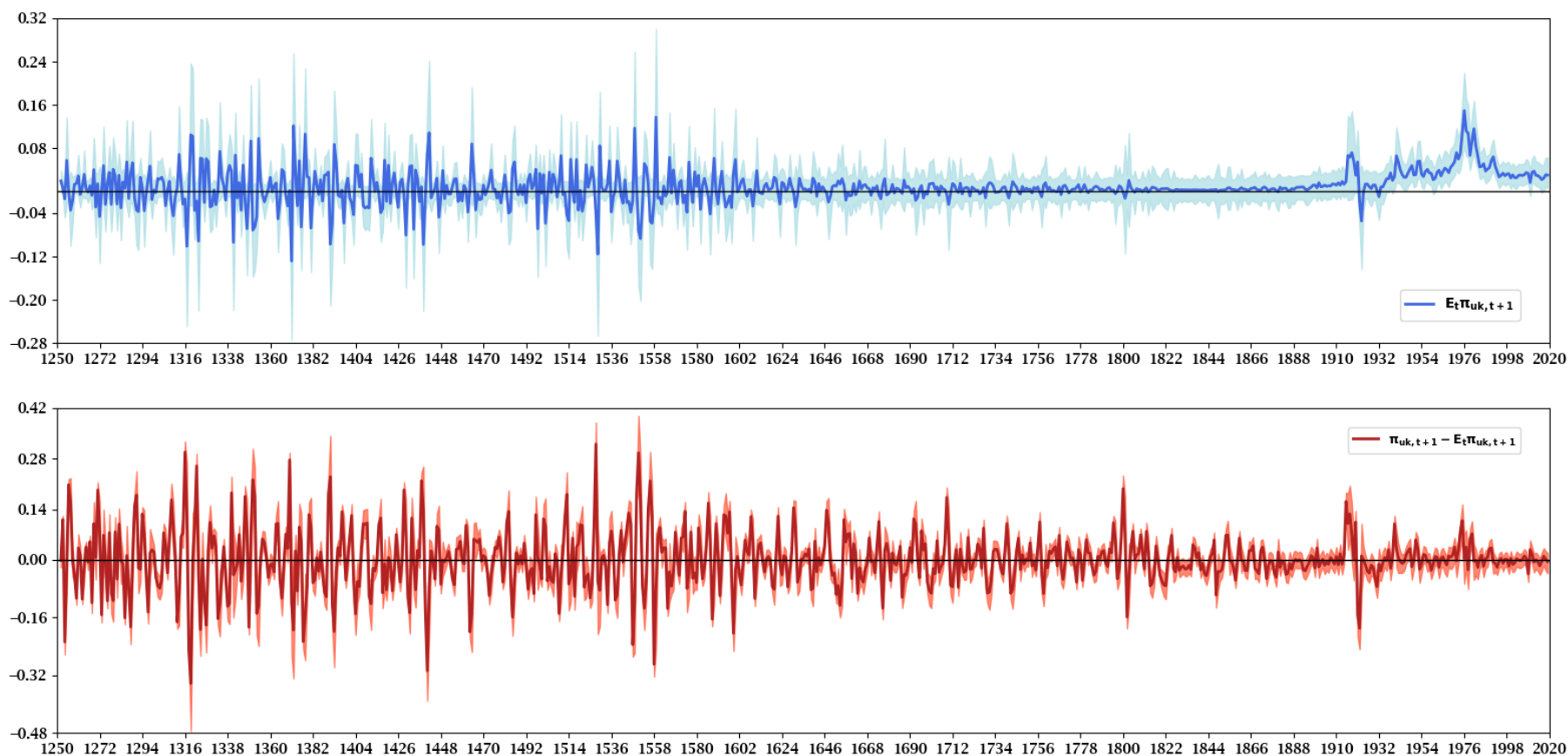
Notes: The top row of panels display the prior and posterior densities of the scale volatilities $\sigma_{\tau,u}^2$, $\tau = 1251-1869, 1870-1914$, and $1915-1946$. The densities are constructed using a normal kernel and methods described by Silverman (1986). Posterior densities are the solid (olive) lines. The (turquoise) dot-dash lines are densities of the prior distributions. The latter distributions are simulated using the priors for the $\sigma_{\tau,u}^2$ s listed in table B1. The median of the posterior of smoothed measurement error, m_t , is the solid (red) line in the bottom left panel. Surrounding m_t are (pink) shadings, which are 68% uncertainty bands. The bottom right panel plots $\pi_{uk,t}$, as the solid green line, the median of the posterior of true inflation, π_t , is the dotted (magenta) line, and (orchid) shadings represent 64% confidence bands.

Figure B2: Posterior Moments of the TVP-SV-AR(3) on UK Inflation, 1251–2019



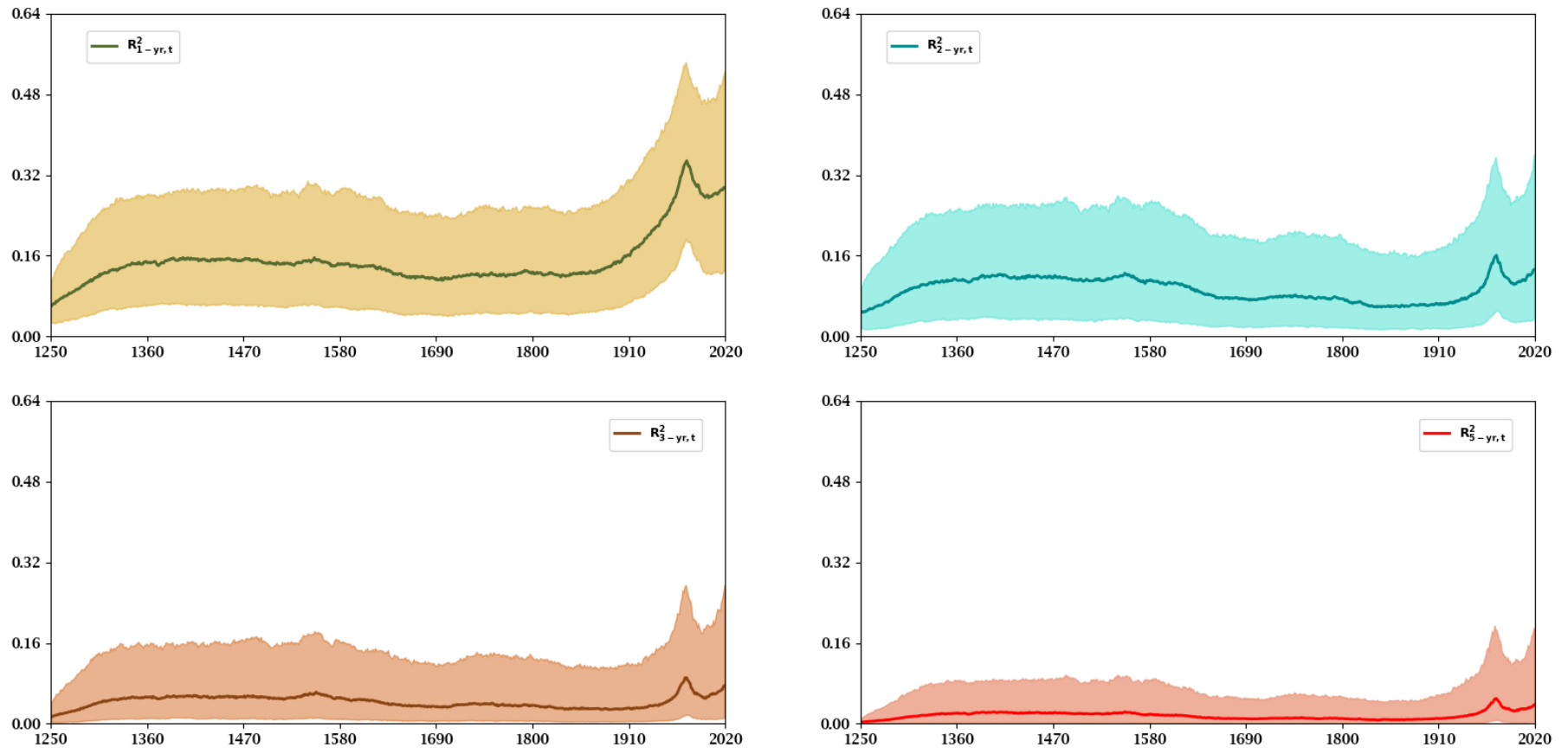
Notes: The top left panel contains the posterior median of the time-varying intercept, $\alpha_{0,t}$. The posterior median of the sum of the lag TVPs, $\sum_{\ell=1}^3 \alpha_{\ell,t}$, is found in the top right panel. A plot of the time-varying conditional mean of UK inflation is depicted in the bottom left panel as the posterior median of $\mu_{\pi,t} = \alpha_{0,t} / (1 - \sum_{\ell=1}^3 \alpha_{\ell,t})$. The SV of UK inflation is displayed in the bottom right panel. The four panels also display shadings that are 68% Bayesian credible sets (*i.e.*, 16% and 84% quantiles) of the TVPs and SV.

Figure B3: 1-Year Ahead Expected UK Inflation and Its Ex Post Forecast Error, 1251–2019



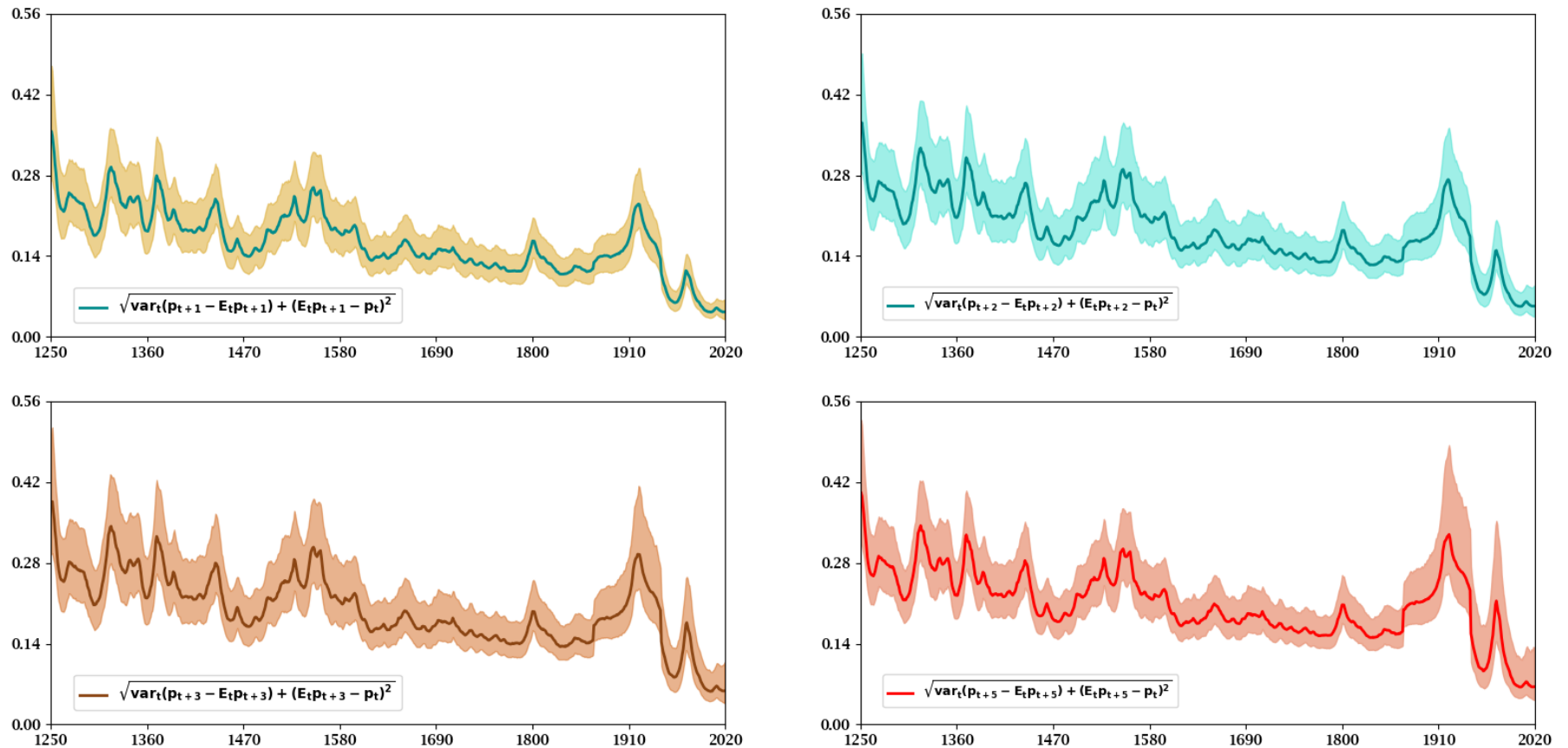
Notes: The top panel plots median 1-year ahead expected UK Inflation, $E_t\pi_{uk,t+1}$. Expected inflation is estimated using the Kalman filter, $\pi_{uk,t}$, and the posterior distribution of the TVP-SV-AR(3) with measurement error. The bottom panel contains the ex post forecast error, $\pi_{uk,t+1} - E_t\pi_{uk,t+1}$. The panels also contain shadings that are 90% Bayesian credible sets (*i.e.*, 5% and 95% quantiles).

Figure B4: Predictability of UK Inflation 1-, 2-, 3-, and 5-Years Ahead, 1251–2019



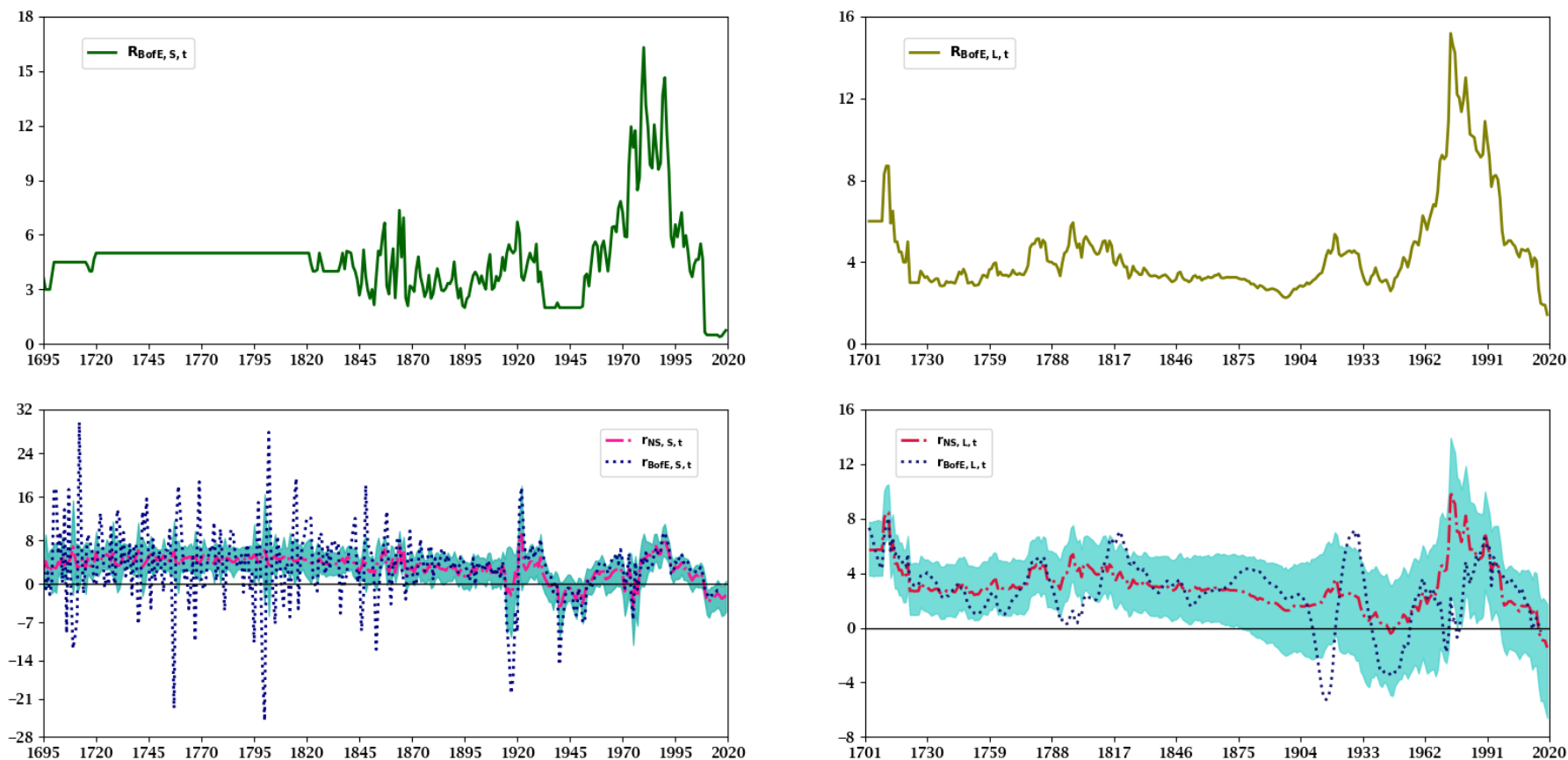
Notes: The top left panel plots the median 1-year ahead R-square statistic, R^2_{1t} , which is computed as described in appendix D, from 1251 to 2019. The shadings around R^2_{1t} are 68% Bayesian credible sets. Similarly, median R^2_{2t} , R^2_{3t} , and R^2_{5t} appear in the top right, bottom left, and bottom right panels along with 68% Bayesian credible sets as the shadings. The R^2_{ht} statistics are computed using the posterior distribution of the TVP-SV-AR(3) with measurement error.

Figure B5: UK Price-Level Instability, 1251–2019



Notes: The top left panel plots the median of the 1-year ahead square root of the sum of the conditional variance and the squared, conditional mean, $\sqrt{\text{var}_t(p_{uk,t+1} - E_t p_{uk,t+1}) + (E_t p_{uk,t+1} - p_{uk,t})^2}$, from 1251 to 2019; see section 5.4 and appendix E for details. The shadings around this statistic are 90% Bayesian credible sets. The median 2-, 3-, and 5-year ahead price-level stability statistics are displayed in the top right, bottom left, and bottom right panels along with shadings that are 68% Bayesian credible sets. The price-level stability statistics are computed using the posterior distribution of the TVP-SV-AR(3) with measurement error.

Figure B6: UK Nominal and Real Short- and Long-Term Interest Rates



Notes: The top row plots UK nominal short- and long-term interest rates; see section 6 for details. The bottom row depicts ex ante short- and long-term real rates, $r_{NS,i,t} = R_{BofE,i,t} - E_t \pi_{uk,t+1}$, in the left and right panels, where $i = S$ (short) and L (long). The $r_{NS,S,t}$ ($r_{NS,L,t}$) begins in 1695 (1703) and ends in 2019. One-year ahead expected inflation is computed using the posterior distribution of the TVP-SV-AR(3) with measurement error. In the bottom row of panels, the shadings are 90% Bayesian credible sets.

Appendix B.3. The TVP-SV-AR(n) minus Measurement Error

This section reports on a model that omits measurement error. Hence $\pi_{uk,t} = \pi_t$, which reduces the model for estimation to equations (3)–(5) of the paper. The last two rows of Table B5 presents the ln MDDs and WAICs for this model. These ln MDDs and WAIC point to different lag lengths for the TVP-SV-AR(n). The data give very strong support to $n = 4$, according to the row of ln *MDDs* in the bottom half of Table B5. In its last row, the WAICs indicate the 1-year ahead forecast error is minimized at $n = 5$.

We also report ln MDDs and WAICs for the baseline model of iid measurement error in the top half of Table B5. These rows reproduce Table 4 of the paper. Including these statistics are useful for comparing the baseline model of iid measurement error with the pure TVP-SV-AR(4) of equations (3)–(5). Table B5 gives decisive evidence the data favor the ARs that lack measurement error to the baseline model of iid measurement error in which $n = 3$, or for any lag length. The former TVP-SV-ARs also offers substantially lower 1-year ahead forecast error as signaled by its WAIC. The explanation is the measures of fit penalize the additional parameters in Ψ of the baseline model of iid measurement error. The information about the breaks in the construction of the data in 1870, 1915, and 1947 fail to improve the fit of the baseline model of iid measurement error compared with the TVP-SV-AR(n)s under the restriction $\pi_{uk,t} = \pi_t$. As a result, measured SV, which is declining during the sample, reflects some of the measurement error in $\pi_{uk,t}$.

Figures B7 to B11 contain results of estimating the TVP-SV-AR(4), given $\pi_{uk,t} = \pi_t$. These results lead to economic conclusions that are quite similar compared with Figures 4–8 generated by the posterior of the baseline model of iid measurement error in the paper. Hence a complete discussion of the results for the TVP-SV-AR(5) in which $\pi_{uk,t} = \pi_t$ is left to our earlier working paper, Nason and Smith (2021).

There are, however, several, numerical similarities and differences across Figures 4 to 8 and Figures B7 to B11 that are worth describing. There is substantial uncertainty surrounding the median of the posterior of $\alpha_{0,t}$ from 1289 to 1921 in the upper left panel of Figure B7. The upper right panel of this figure displays wider Bayesian credible sets of the posterior $\sum_{i=1}^4 \alpha_{i,t}$ during the sample compared with the same panel in Figure 3. These Bayesian credible sets do not include zero year by year from the 1251 to 1649. This

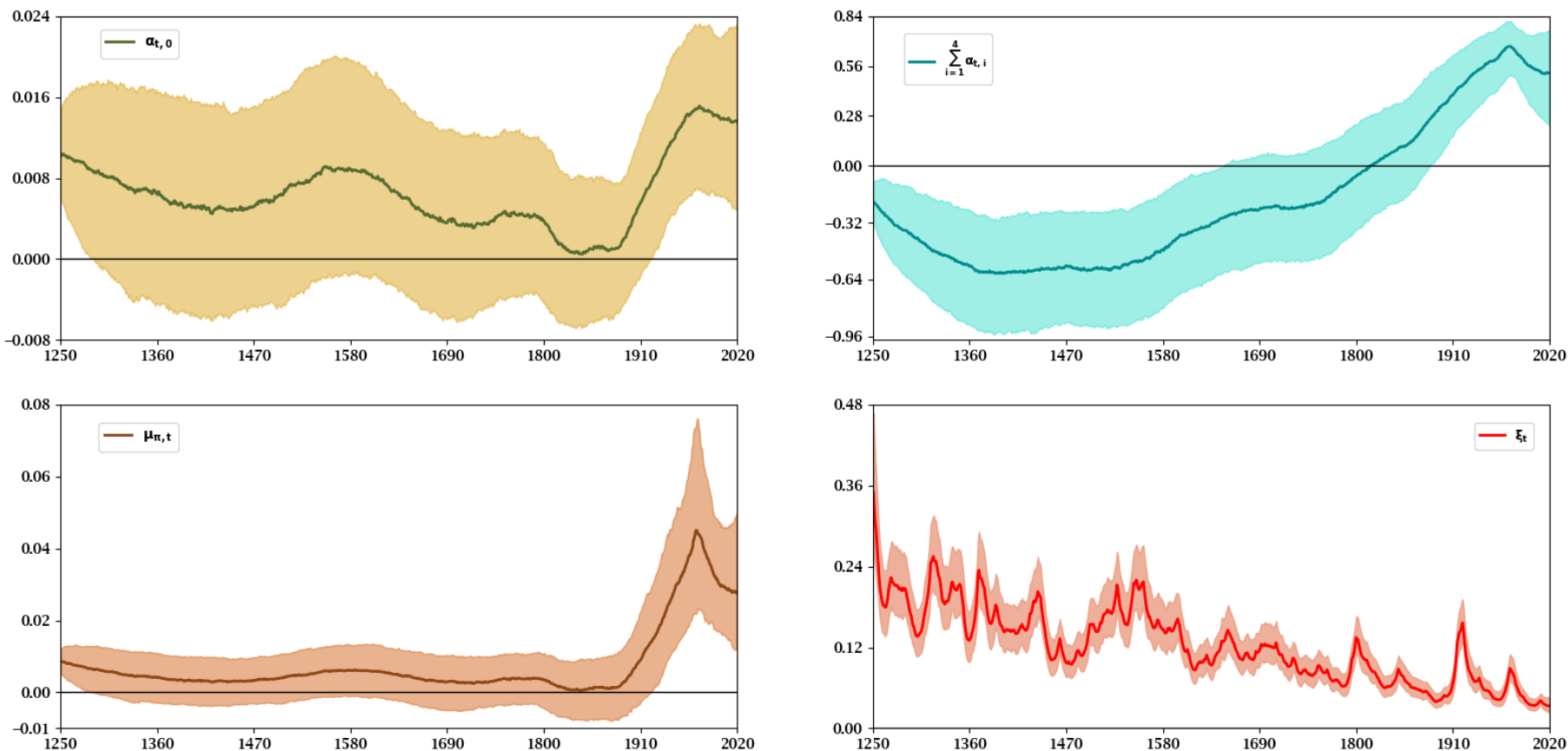
sum reaches its trough at 0.61 in 1398 and hits its peak at 0.67 in 1975. In the lower left panel of Figure B7, the posterior median estimate of $\mu_{\pi,t}$ peaks at 4.50% in 1974. The associated Bayesian credible sets cover zero year by year from 1289 to 1921. Hence, evidence of a single great wave of inflation in the 20th century is reinforced by estimates of the TVP-SV-AR(4) that lack measurement error, $\pi_{uk,t} = \pi_t$. The lower right panel of this figure shows that SV declines throughout the sample with local peaks in 1251, 1319, 1371, 1550, 1597, and 1921. Figure B8 contains 1-year ahead inflation forecasts and forecast errors that mirror the inflation forecasts that appear in figure 5. The same is true for Figures 6 and Figure B9 with two exceptions. The latter figure shows larger maximum median estimates of the posteriors of R_{ht}^2 at all horizons. These peaks are 0.43, 0.20, 0.14, and 0.09 at $h = 1, 2, 3,$ and 5 and occur at 1975 for all horizons but 2-years ahead, which is in 1974. The other difference is that at 3- and 5-years ahead the 16th quantiles are well above zero for the entire sample. Figure B9 shows the lower bound of these 68% Bayesian credible sets are no smaller than 0.01 and 0.004 from the early 1300s to the early 1900s. Comparing Figures 7 and B10 reveals similar local peaks in the price stability statistics. The local peaks are 1319, 1371, 1438, 1528, 1550, 1558, 1800, 1921, and 1975 with the largest centered on the early 1300s, 1370s, mid 1550s, 1917-1922, and mid 1970s. Plots of the posteriors of short-term and long-term real interest rates in the bottom row of Figures 8 and B11 are also qualitatively similar. However, the 90% Bayesian credible sets are narrower in Figure B11. Moreover, not modeling measurement error raises the maximum median short-term real interest rate by 60 basis points to 12.3% in 1922, but the maximum median long-term real interest rate is lowered by about 40 basis points to 10.7% in 1974.

**Table B5: Comparison of Fit of the TVP-SV-AR(n)s
without Measurement Error**

	AR(1)	AR(2)	AR(3)	AR(4)	AR(5)	AR(6)
Baseline:						
ln MDD	638.21	643.18	673.62	667.59	652.72	650.82
WAIC	-1431.95	-1457.55	-1487.87	-1483.30	-1487.75	-1465.82
No Measurement Error:						
ln MDD	764.56	780.20	801.46	817.51	813.47	806.85
WAIC	-1634.70	-1661.84	-1704.80	-1714.75	-1719.75	-1715.24

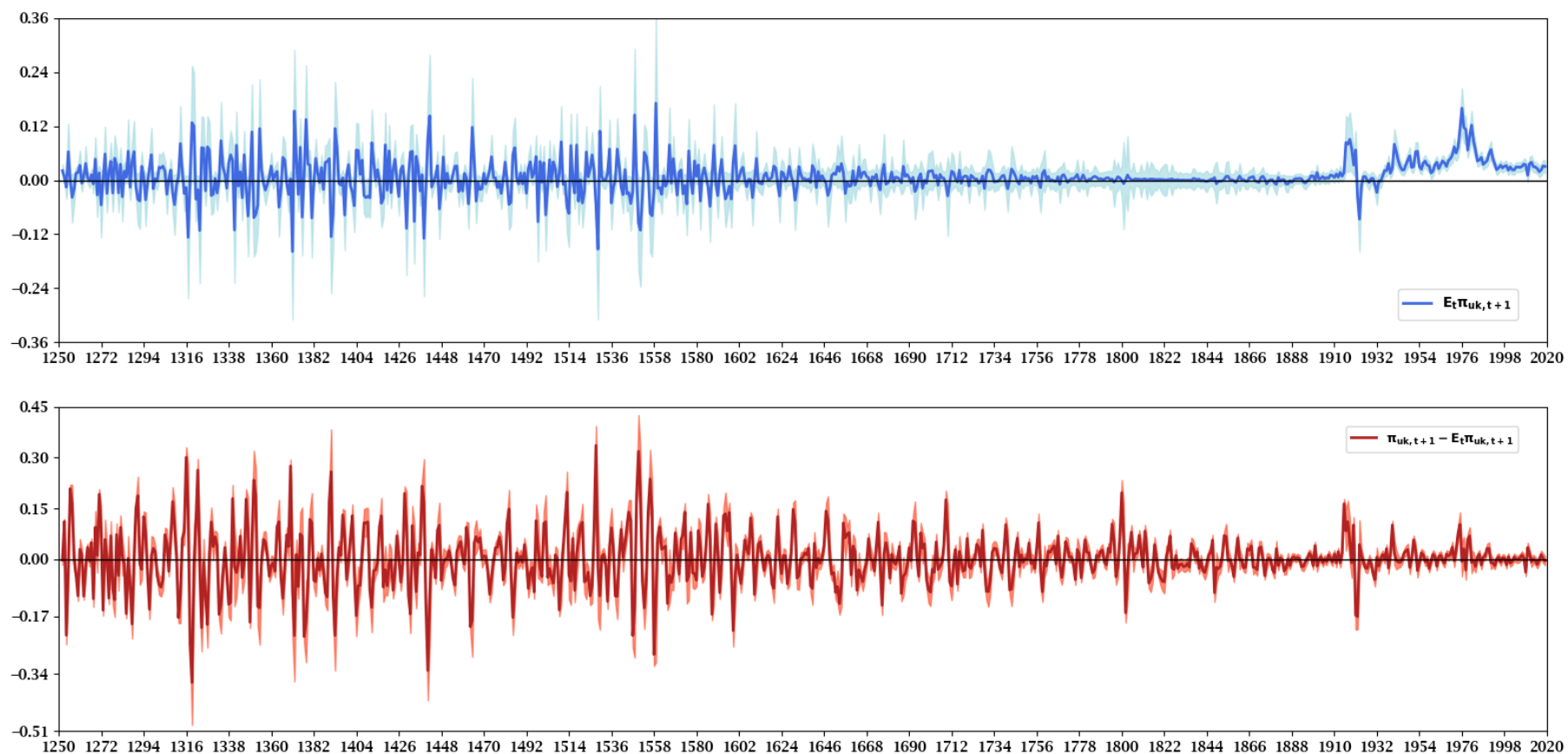
Notes: The first two lines reproduce Table 4 in the paper for our baseline model of measurement error. The final two rows contain the ln MDDs and WAICs for the posteriors of TVP-SV-AR(n)s of equations (3)-(5) alone, which exclude measurement error implying $\pi_{u_{k,t}} = \pi_t$. See Table 3 of the paper for the priors on the initial conditions of α_0 , Ω_η , and $\ln \xi_0^2$.

Figure B7: Posterior Moments of the TVP-SV-AR(4) on UK Inflation, 1251–2019



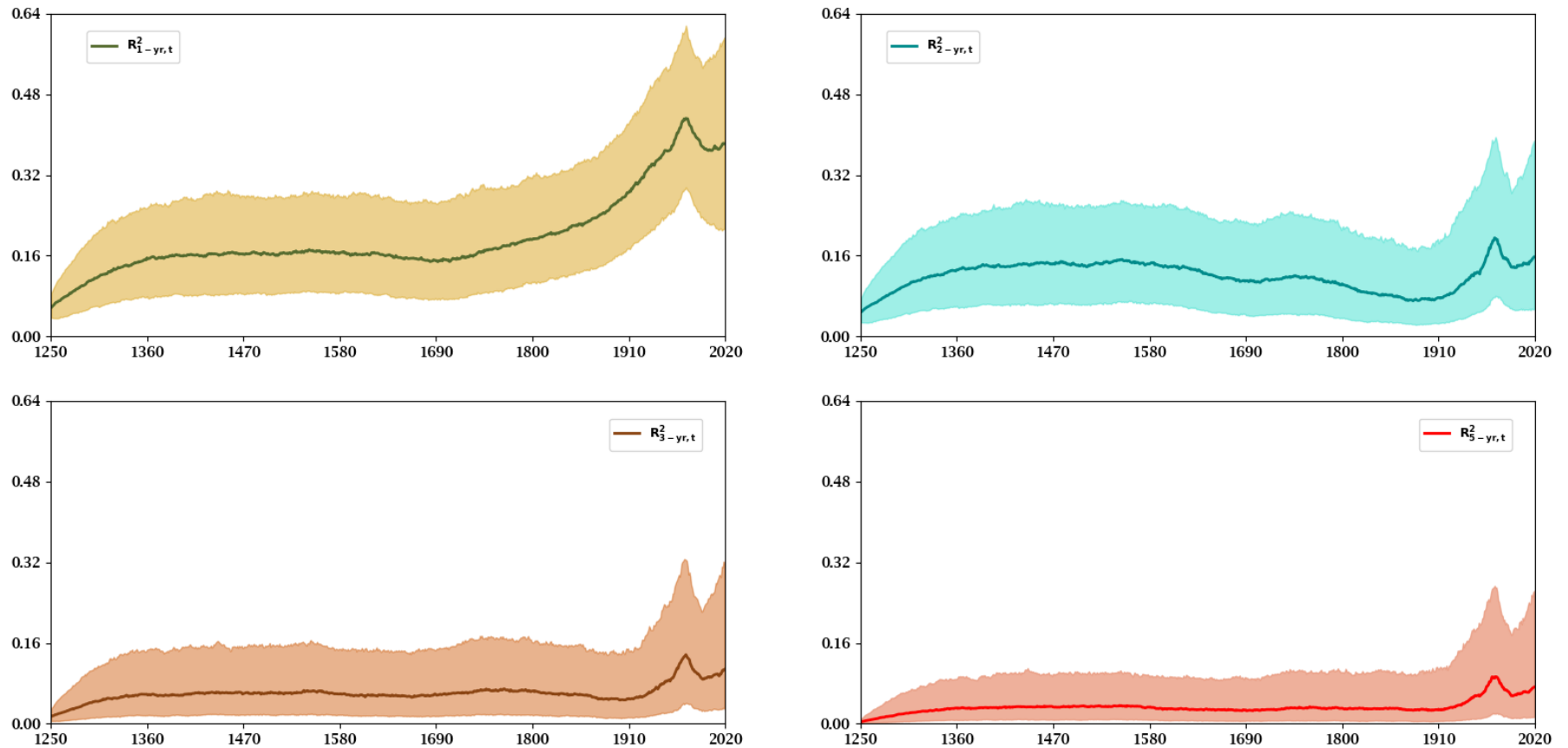
Notes: The top left panel contains the posterior median of the time-varying intercept, $\alpha_{0,t}$. The posterior median of the sum of the lag TVPs, $\sum_{\ell=1}^4 \alpha_{\ell,t}$, is found in the top right panel. A plot of the time-varying conditional mean of UK inflation is depicted in the bottom left panel as the posterior median of $\mu_{\pi,t} = \alpha_{0,t} / (1 - \sum_{\ell=1}^4 \alpha_{\ell,t})$. The SV of UK inflation is displayed in the bottom right panel. The four panels also display shadings that are 68% Bayesian credible sets (*i.e.*, 16% and 84% quantiles) of the TVPs and SV.

Figure B8: 1-Year Ahead Expected UK Inflation and Its Ex Post Forecast Error, 1251–2019



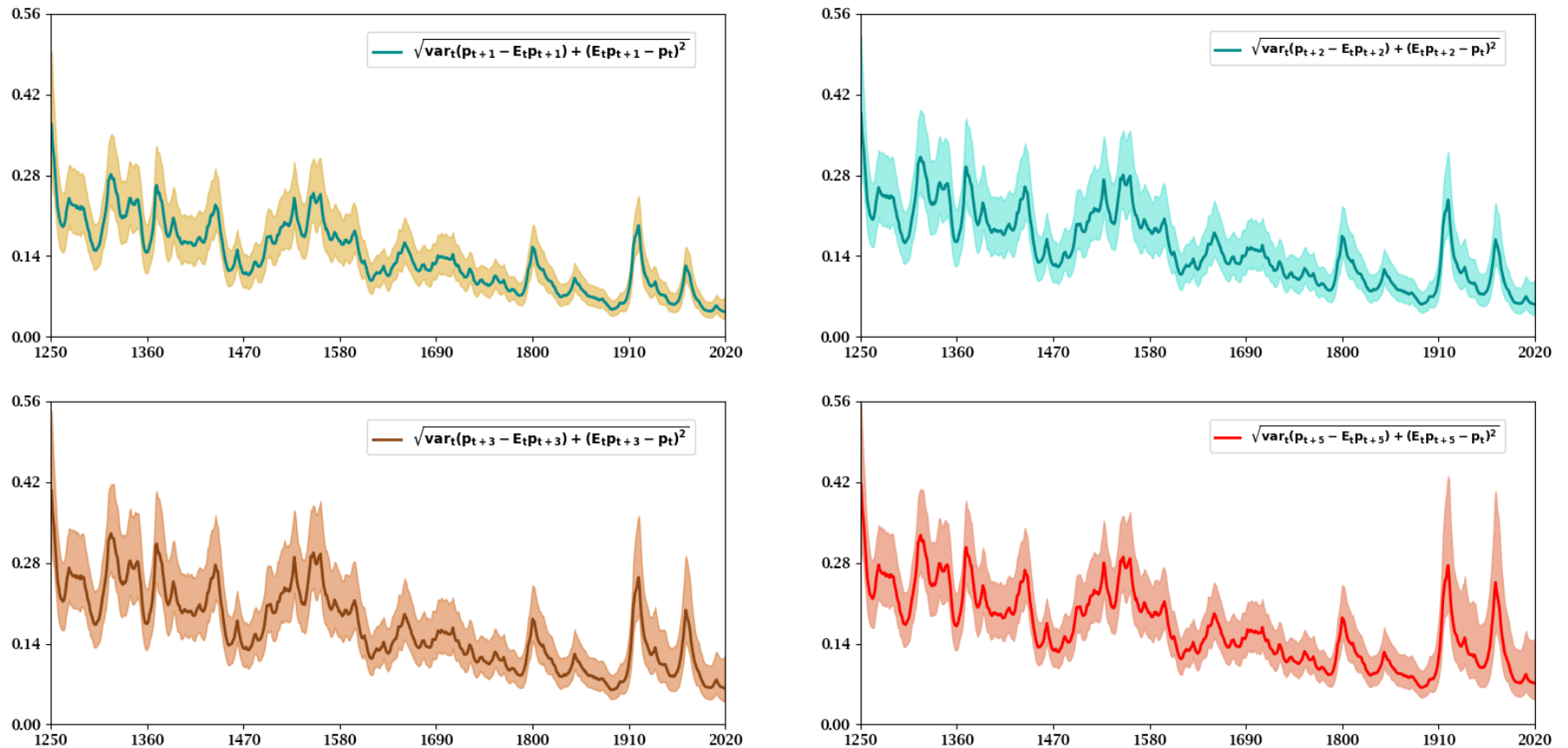
Notes: The top panel plots median 1-year ahead expected UK Inflation, $E_t \pi_{uk,t+1}$. Expected inflation is estimated using the Kalman filter, sample UK inflation, and the posterior distribution of the TVP-SV-AR(4). The bottom panel contains the ex post forecast error, $\pi_{uk,t+1} - E_t \pi_{uk,t+1}$. The panels also contain shadings that are 90% Bayesian credible sets (*i.e.*, 5% and 95% quantiles).

Figure B9: Predictability of UK Inflation 1-, 2-, 3-, and 5-Years Ahead, 1251–2019



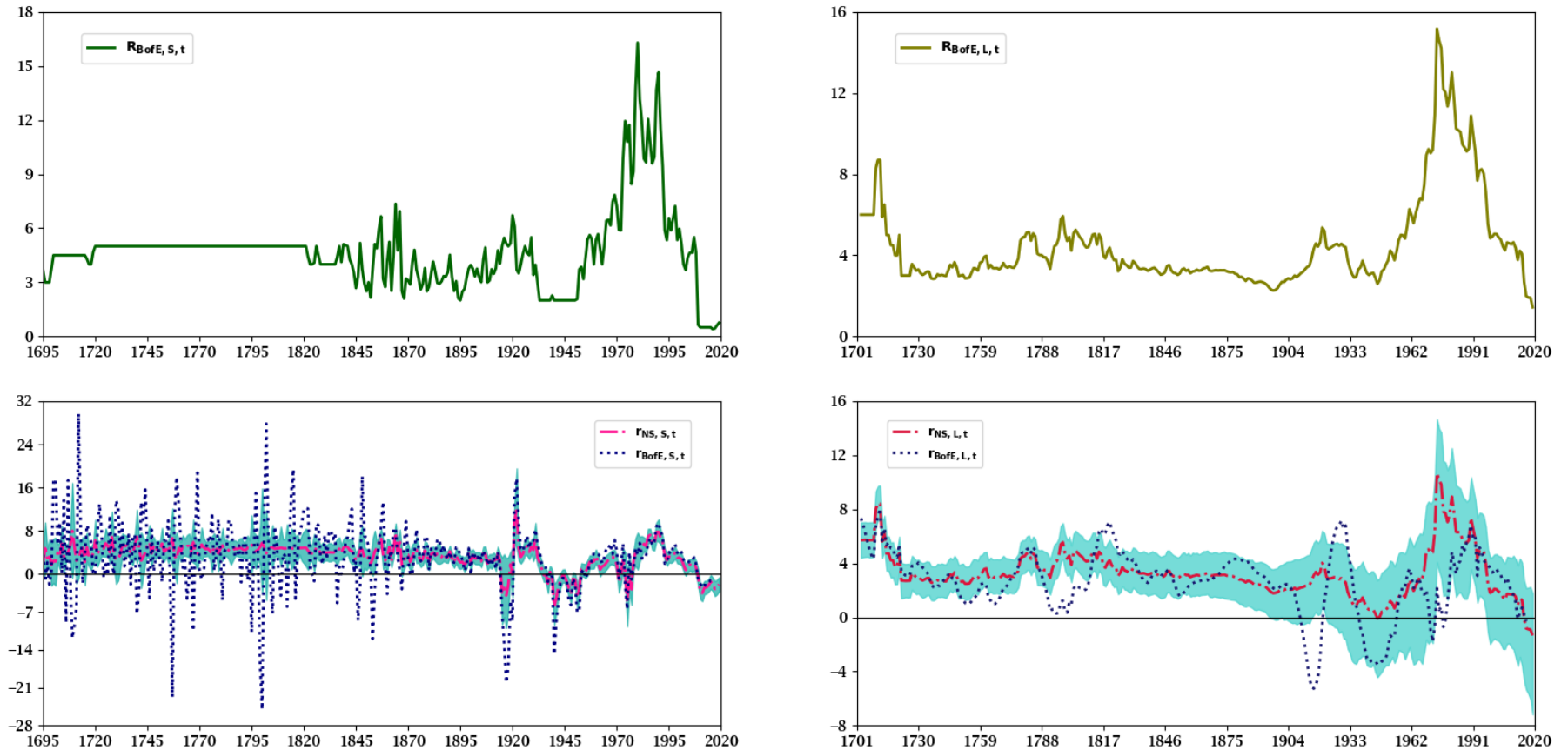
Notes: The top left panel plots the median 1-year ahead R-square statistic, R^2_{1t} , which is computed as described in appendix D, from 1251 to 2019. The shadings around R^2_{1t} are 68% Bayesian credible sets. Similarly, median R^2_{2t} , R^2_{3t} , and R^2_{5t} appear in the top right, bottom left, and bottom right panels along with 68% Bayesian credible sets as the shadings. The R^2_{ht} statistics are computed using the posterior distribution of the TVP-SV-AR(4).

Figure B10: UK Price-Level Instability, 1251–2019



Notes: The top left panel plots the median of the 1-year ahead square root of the sum of the conditional variance and the squared conditional mean, $\sqrt{\text{var}_t(p_{uk,t+1} - E_t p_{uk,t+1}) + (E_t p_{uk,t+1} - p_{uk,t})^2}$, from 1251 to 2019; see section 5.4 and appendix E for details. The shadings around this statistic are 90% Bayesian credible sets. The median 2-, 3-, and 5-year ahead price-level stability statistics are displayed in the top right, bottom left, and bottom right panels along with shadings that are 68% Bayesian credible sets. The price-level stability statistics are computed using the posterior distribution of the TVP-SV-AR(4).

Figure B11: UK Nominal and Real Short- and Long-Term Interest Rates



Notes: The top row plots UK nominal short- and long-term interest rates; see section 6 for details. The bottom row depicts ex ante short- and long-term real rates, $r_{NS,i,t} = R_{BofE,i,t} - E_t \pi_{uk,t+1}$, in the left and right panels, where $i = S$ (short) and L (long). The $r_{NS,S,t}$ ($r_{NS,L,t}$) begins in 1695 (1703) and ends in 2019. One-year ahead expected inflation is computed using the posterior distribution of the TVP-SV-AR(4). In the bottom row of panels, the shadings are 90% Bayesian credible sets.

Appendix B.4. The Horseshoe Prior

This section discusses a TVP-SV-AR(n) without measurement error that replaces the fixed variance, σ_ϕ^2 , of the innovation to SV, ϕ_t with an alternative prior that allows for the variance to be time-varying. A motivation is the critique that the random walk specification of the states of a TVP-SV-VAR generate drift that might obscure sudden breaks in these variables by imposing smooth and slow adjustment. Results in the paper and Appendices B.1, B.2 and B.3 assume random walk drift in α_t ($\ln \xi_t^2$) that have (has) homoscedastic innovations with a covariance matrix drawn from an \mathcal{IW} (variance from an \mathcal{IG}) prior. Hence, we use this section as robustness check on results presented in the paper and elsewhere in the Appendix, but only with respect to the SV.

One approach to introducing time-variation in σ_ϕ^2 is the horseshoe prior. It has been suggested as an alternative to an \mathcal{IG} prior on a scale parameter. We work with the horseshoe prior of Carvalho, Polson, and Scott (2010) and Polson and Scott (2012). They tie the horseshoe prior to the half-Cauchy distribution, which truncates a Cauchy distribution with location and scale parameters set to zero and one to the non-negative part of the real line, $\mathcal{HC}(0, 1 | 0, \infty)$. In the VAR literature, an example is Prüser (2021). He advocates replacing the \mathcal{IG} prior on the fixed variances of the innovations of the TVPs and SVs of a structural VAR with the horseshoe prior. The comparison is with an \mathcal{IG} prior because Prüser assumes, along with Bitto and Frühwirth-Schnatter (2019), Follett and Yu (2019), and Cadonna, Frühwirth-Schnatter, and Knaus (2020), that the covariance matrix of innovations to the TVPs is diagonal.

We adapt the horseshoe prior of Prüser (2021) to our TVP-SV-AR(n)s, but only for SV, $\ln \xi_t^2$. One reason is that plots of the medians of the posterior of $\alpha_{0,t}$ and $\sum_{i=1}^n \alpha_{i,t}$ in Figure 5 indicate that the standard \mathcal{IW} prior is more than capable of capturing rapid changes in these TVPs conditional on the UK inflation data and our priors. Moreover, the posterior of the baseline model of measurement error produce draws of Ω_η with off-diagonal elements that show innovations to the elements of α_t have non-zero correlation. We argue this posterior correlation is economically more important than the benefits of time-varying heteroscedasticity in the independent random walks of the TVPs.

Table B6 presents our horseshoe prior for time-varying heteroscedasticity in the in-

novation of $\ln \xi_t^2$. The horseshoe prior, as implemented by Prüser (2021), allows for heteroscedasticity in ϕ_t by assuming its variance is decomposed into static or global and local or time-varying components, $\sigma_{\phi,t}^2 = \psi^{-2}\zeta_t^2$, where $\psi, \zeta_t \sim \mathcal{HC}(0, 1|0, \infty)$.

Prüser relies on Makalic and Schmidt (2016) to map the unconditional $\mathcal{HC}(0, 1|0, \infty)$ prior into a conditional posterior composed of a scale mixture of four \mathcal{IG} distributions. They devise a procedure to make conditionally independent posterior draws. The sequence of posterior draws starts by obtaining a new realization of the global component ψ^2 conditional on $\ln \xi^{2T}$, the local component ζ_t^2 , and δ_ψ , which is the previous draw of the precision (*i.e.* inverse of the scale) parameter of the \mathcal{IG} posterior distribution of ψ^2 . Next, a similar draw updates ζ_t conditional on the previous draws of $\ln \xi_t^2$, $\ln \xi_{t-1}^2$, ζ_t^2 , and δ_ζ , which is the previous draw of the precision parameter of the \mathcal{IG} posterior distribution of ζ_t^2 . Last, δ_ψ and δ_ζ are updated by drawing from the \mathcal{IG} posterior distributions in which the precision parameters $\psi^2/(1 + \psi^2)$ and $\zeta_t^2/(1 + \zeta_t^2)$ employ the most recent updates.

Implementing the horseshoe prior alters step 2 of the MH in Gibbs MCMC sampler described in Appendix C in two ways. First, initial draws of ψ^2 , ζ_0^2 , δ_ψ , and δ_ζ from \mathcal{IG} priors replace the initial draw of σ_ϕ^2 . These \mathcal{IG} priors are grounded in the revised horseshoe ordering between equations (6) and (7) of Makalic and Schmidt (2016). Second, step 2c) of the MCMC sampling algorithm of Appendix C is altered to account for the conditionally independent posterior draws discussed previously and outlined in Table B6.

Table B7 evaluates the fit of the TVP-SV-AR(n)s with the horseshoe prior. For simplicity, we apply this model directly to $\pi_{uk,t}$ and omit the 4-span treatment of measurement error. Both the \ln MDD and WAIC criteria suggest a lag length of $n = 6$ years. For comparison, Table B7 also repeats the same statistics for the TVP-SV-AR(n)s minus measurement error with the priors of Table 3 in the paper that endow σ_ϕ^2 with an \mathcal{IG} prior. Overall, these statistics yield evidence on whether the data throws more support to the TVP-SV-AR(6) reported on Table B7 or the TVP-SV-AR(4) of Table B5 that is hardly worth mentioning. The gap in the WAICs is less than one showing both models produce similar predictive loss at the 1-year horizon. Thus invoking a horseshoe prior on $\sigma_{\phi,t}^2$ does not result in TVP-SV-AR(n)s restricted by $\pi_{uk,t} = \pi_t$ that receive more support from the data or are superior forecasting models. Hence the horseshoe prior does not alter

the evidence that TVP-SV-AR(n)s lacking in measurement error dominate our baseline model of iid measurement error.

Figures B12–B16 contain results from the TVP-SV-AR(6) with the horseshoe prior on SV in which $\pi_{uk,t} = \pi_t$ that again are similar to those in Figures 4–8 of the paper. There are, however, several, numerical similarities and differences across Figures 4 to 8 and B12 to B16 that are worth describing. First, there is less uncertainty surrounding the median of the posterior of $\alpha_{0,t}$ during the sample. For example, only from 1329 to 1910 do the 68% Bayesian credible sets include zero year by year in the upper left panel of Figure B12. The upper left panel of Figure 4 shows this interval starts in 1261 (68 years earlier) and ends on 1923 (13 years later) for the baseline model of iid measurement error. Second, the upper right panel of Figure B12 displays wider Bayesian credible sets of the posterior $\sum_{i=1}^6 \alpha_{i,t}$ from the mid 1300s to the mid 1600s compared with the same panel in Figure 4. This plot has a trough in 1353 at -0.46 and peaks at 0.62 in 1974 while in Figure B12 the trough occurs later, in 1486, at -0.61, but the peak of 0.69 is in the same year. Third, the posterior median estimate of $\mu_{\pi,t}$ peaks at 3.50% in 1977 as appears in the lower left panel of Figure B12. This is two years after and almost a third less than the same estimate of 5.06% produced by the baseline model of iid measurement error that we report in the paper. Next, the lower right panel of this figure shows that SV declines throughout the sample with local peaks in 1251, 1319, 1371, 1558, and 1921. The 1-year ahead inflation forecasts and forecast errors of Figure B13 closely resemble the inflation forecasts that appear in Figure 5. Fifth, the same is true for Figures 6 and B14, but the latter shows larger maximum estimates of the posteriors of R_{ht}^2 at $h = 2, 3,$ and 5 all in 1975. Sixth, comparing Figures 7 and B15 reveals that employing the horseshoe prior places the local peaks of the price stability statistics in the same years. However, the peaks focused on 1917–1922 and 1975 dominate when using the horseshoe prior. Finally, posterior estimates of short-term and long-term real interest rates are similar across Figures 8 and B16. However, the horseshoe prior results in a 120 basis point increase to 12.9% in the maximum of the median of the posterior of the short-term real rate in 1922 and a 60 basis point increase to 11.7% in the maximum of the median of the posterior of the long-term real interest rate in 1974.

Table B6: Horseshoe Prior on the SV of the TVP-SV-AR(n)s

$$\begin{aligned} \pi_t &= \alpha_{0,t} + \sum_{i=1}^n \alpha_{i,t} \pi_{t-i} + \xi_t \epsilon_t, & \epsilon_t &\sim \mathcal{N}(0, 1), \\ \alpha_t &\equiv \{\alpha_{0,t}, \alpha_{1,t}, \alpha_{2,t}, \dots, \alpha_{n,t}\}, \\ \alpha_t &= \alpha_{t-1} + \eta_t, & \eta_t &\sim \mathcal{N}(0_{n+1}, \Omega_\eta), \\ \ln \xi_t^2 &= \ln \xi_{t-1}^2 + \sigma_{\phi,t} \phi_t, & \phi_t &\sim \mathcal{N}(0, 1), \\ \sigma_{\phi,t}^2 &= \psi^{-2} \zeta_t^2, & \psi, \zeta_t &\sim \mathcal{HC}(0, 1 | 0, \infty). \end{aligned}$$

Conditionally Independent Draws	Posterior Distribution	Parameters	
		θ_1	θ_2
$\psi^2 \mid \ln \xi_t^2, \delta_\psi, \zeta_t^2$	\mathcal{IG}	$\frac{T+1}{2}$	$\sigma_{\xi,T}^2 + 1/\delta_\psi$
$\zeta_t^2 \mid \ln \xi^{2T}, \ln \xi_0^2, \delta_\zeta, \psi^2$	\mathcal{IG}	1	$\sigma_{\xi,t}^2 + 1/\delta_\zeta$
$\delta_\psi \mid \psi^2$	\mathcal{IG}	1	$1 + 1/\psi^2$
$\delta_\zeta \mid \zeta_t^2$	\mathcal{IG}	1	$1 + 1/\zeta_t^2$

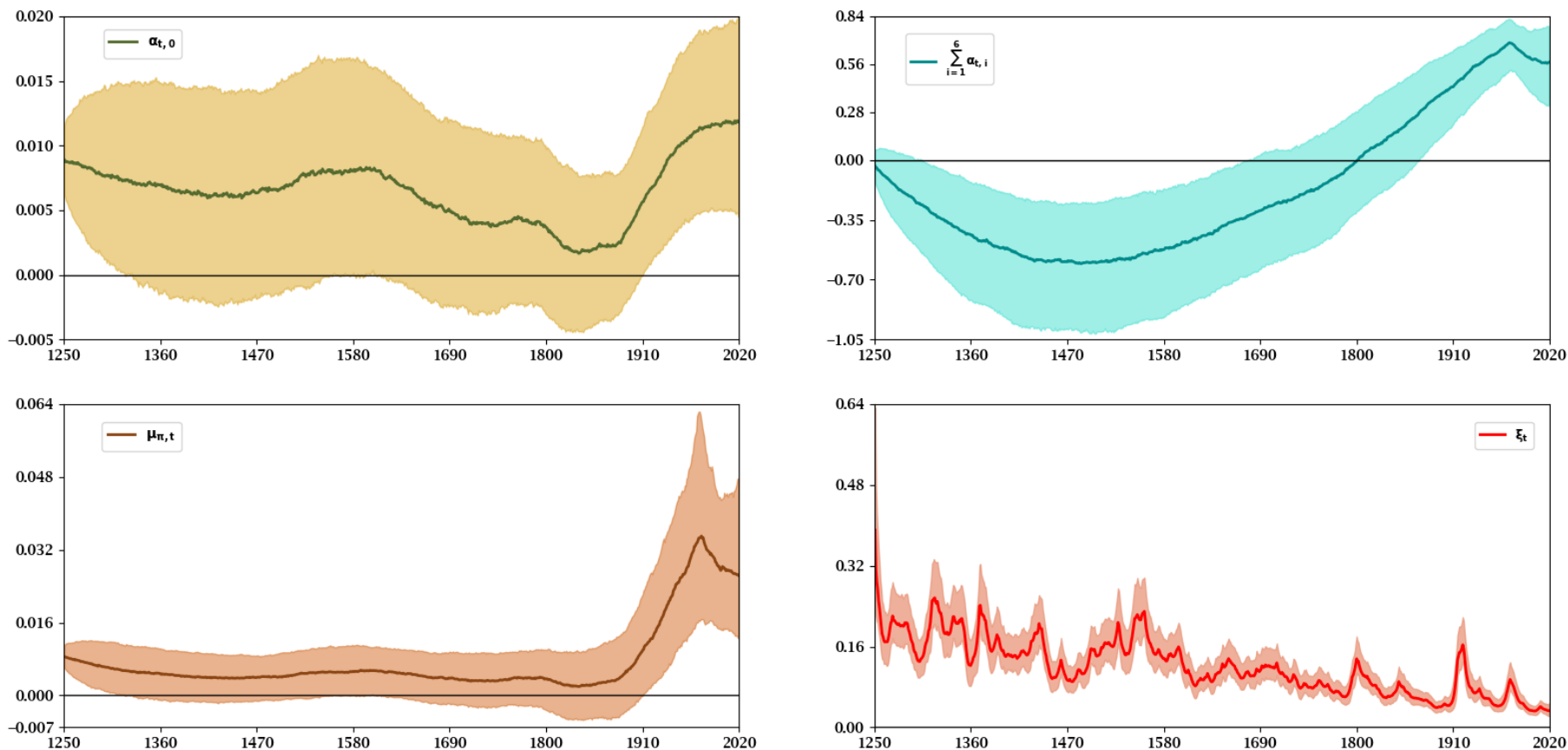
Notes: Makalic and Schmidt (2016) represent the half-Cauchy (\mathcal{HC}) distribution as conditional and unconditional \mathcal{IG} distributions. As discussed in Prüser (2021), this implies for the random variables \mathcal{Y} and λ that conditioning the square of the former on the latter, $\mathcal{Y}^2 \mid \lambda \sim \mathcal{IG}(0.5, 1/\lambda)$ and $\lambda \sim \mathcal{IG}(0.5, 1)$, yields $\mathcal{Y} \sim \mathcal{HC}(0, 1 \mid 0, \infty)$, which is the \mathcal{HC} distribution truncated to the non-negative part of the real line with location and scale parameters $\theta_1 = 0$ and $\theta_2 = 1$. The \mathcal{IG} distribution is parameterized by the shape and scale parameters θ_1 and θ_2 . The draws of ψ^2 and ζ_t^2 require computing $\sigma_{\xi,T}^2 = 0.5 \sum_{t=0}^T (\Delta \ln \xi_t^2)^2 / \zeta_t^2$ and $\sigma_{\xi,t}^2 = 0.5 (\Delta \ln \xi_t^2)^2 / \psi^2$. Otherwise, see Table 3 of the paper for the priors on the initial conditions of α_0 , Ω_η , and $\ln \xi_0^2$.

**Table B7. Evaluation of Fit of the TVP-SV-AR(n)s
with a Horseshoe Prior on SV**

	AR(1)	AR(2)	AR(3)	AR(4)	AR(5)	AR(6)
No Measurement Error:						
ln MDD	764.56	780.20	801.46	817.51	813.47	806.85
WAIC	-1634.70	-1661.84	-1704.80	-1714.75	-1719.75	-1715.24
Horseshoe Prior:						
ln MDD	758.49	778.34	807.13	805.17	809.33	818.40
WAIC	-1620.89	-1669.76	-1696.45	-1710.08	-1708.58	-1718.85

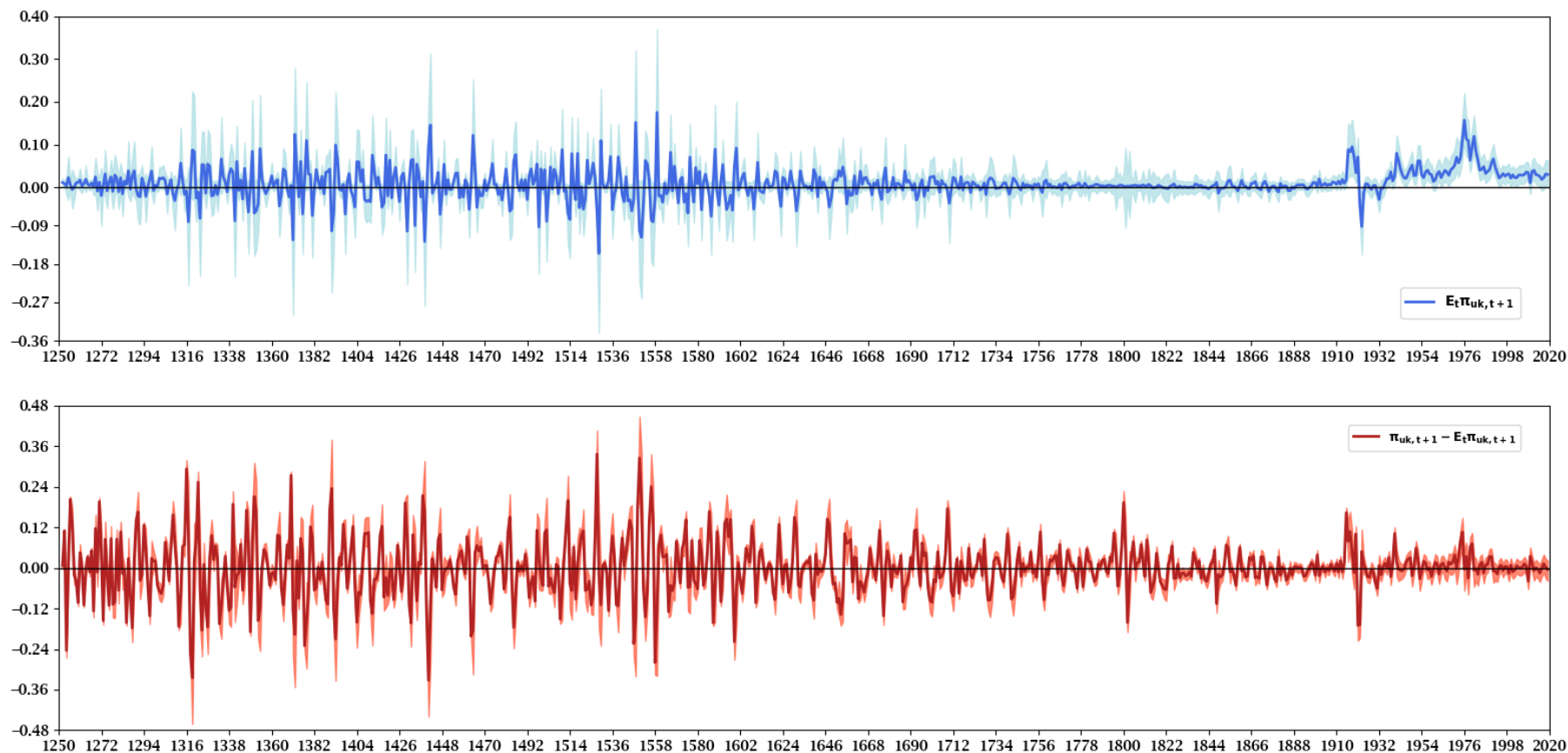
Notes: See the notes to Table 4 of the paper. For simplicity the statistics are calculated directly on $\{\pi_{uk,t}\}$, ignoring measurement error.

Figure B12: Posterior Moments of the TVP-SV-HS-AR(6) on UK Inflation, 1251–2019



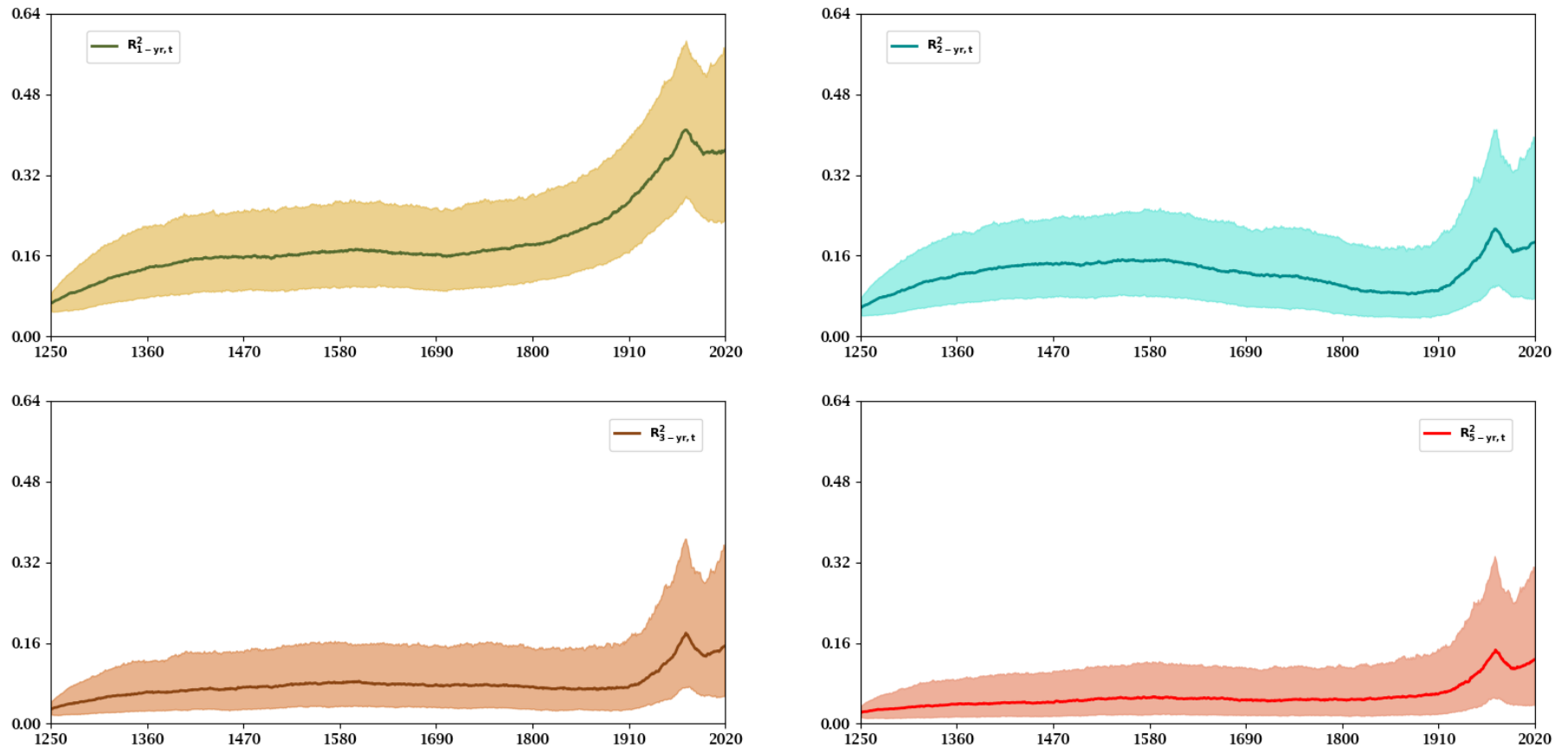
Notes: The top left panel contains the posterior median of the time-varying intercept, $\alpha_{0,t}$. The posterior median of the sum of the lag TVPs, $\sum_{\ell=1}^6 \alpha_{\ell,t}$, is found in the top right panel. A plot of the time-varying conditional mean of UK inflation is depicted in the bottom left panel as the posterior median of $\mu_{\pi,t} = \alpha_{0,t} / (1 - \sum_{\ell=1}^6 \alpha_{\ell,t})$. The SV of UK inflation is displayed in the bottom right panel. The four panels also display shadings that are 68% Bayesian credible sets (*i.e.*, 16% and 84% quantiles) of the TVPs and SV.

Figure B13: 1-Year Ahead Expected UK Inflation and Its Ex Post Forecast Error, 1251–2019



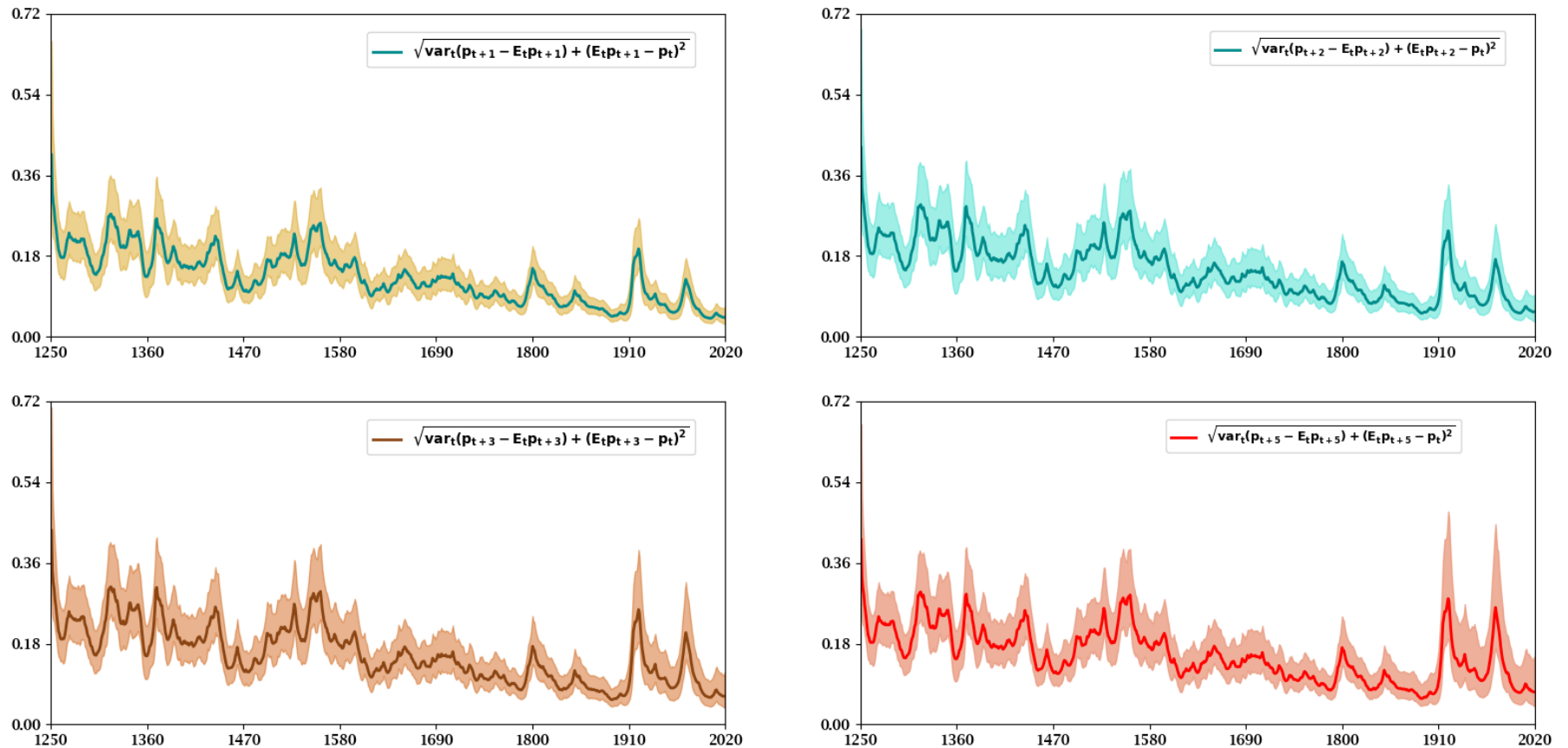
Notes: The top panel plots median 1-year ahead expected UK Inflation, $E_t \pi_{uk,t+1}$. Expected inflation is estimated using the Kalman filter, sample UK inflation, and the posterior distribution of the TVP-SV-HS-AR(6). The bottom panel contains the ex post forecast error, $\pi_{uk,t+1} - E_t \pi_{uk,t+1}$. The panels also contain shadings that are 90% Bayesian credible sets (*i.e.*, 5% and 95% quantiles).

Figure B14: Predictability of UK Inflation 1-, 2-, 3-, and 5-Years Ahead, 1251–2019



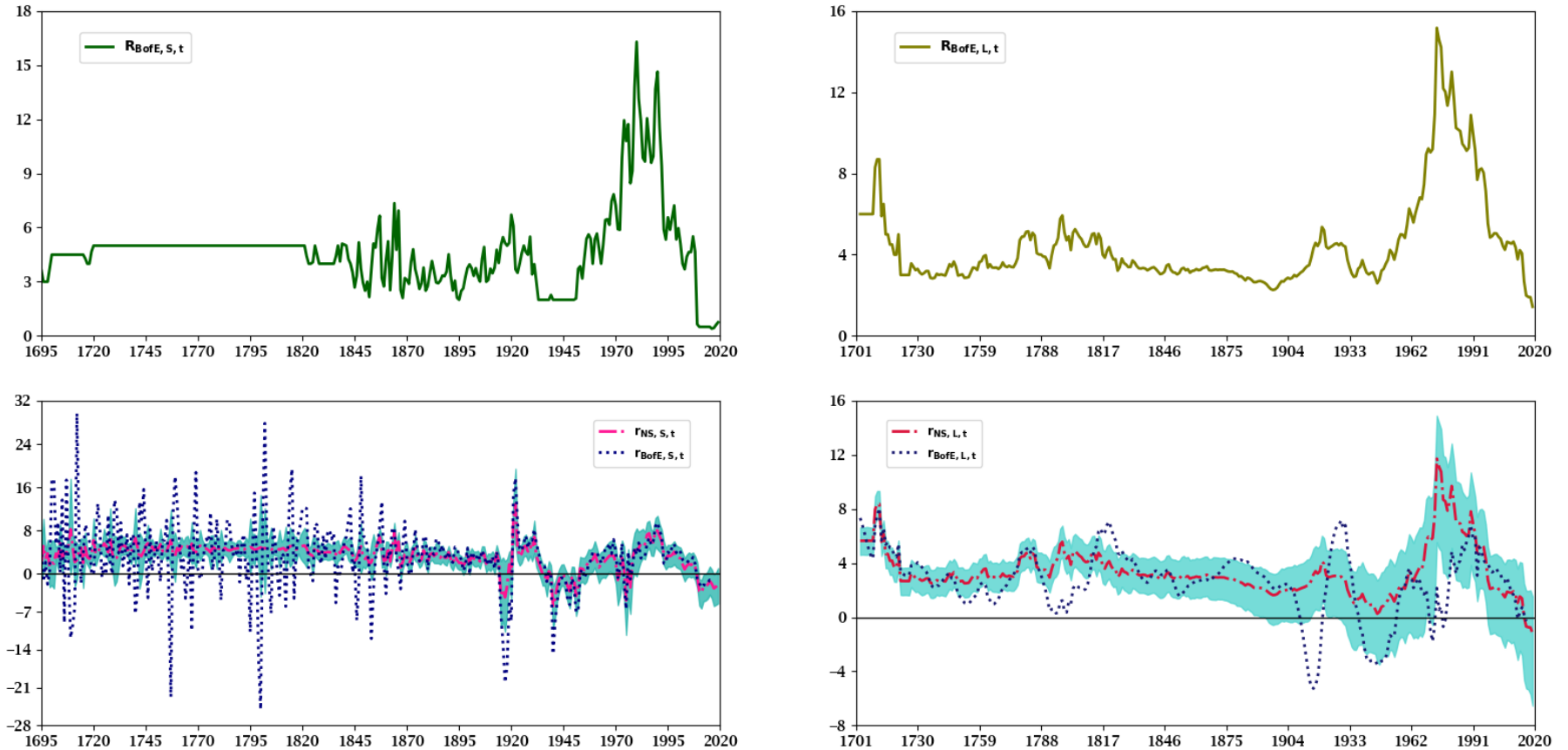
Notes: The top left panel plots the median 1-year ahead R-square statistic, R^2_{1t} , which is computed as described in appendix D, from 1251 to 2019. The shadings around R^2_{1t} are 68% Bayesian credible sets. Similarly, median R^2_{2t} , R^2_{3t} , and R^2_{5t} appear in the top right, bottom left, and bottom right panels along with 68% Bayesian credible sets as the shadings. The R^2_{ht} statistics are computed using the posterior distribution of the TVP-SV-HS-AR(6).

Figure B15: UK Price-Level Instability, 1251–2019



Notes: The top left panel plots the median of the 1-year ahead square root of the sum of the conditional variance and the squared, conditional mean, $\sqrt{\text{var}_t(p_{uk,t+1} - E_t p_{uk,t+1}) + (E_t p_{uk,t+1} - p_{uk,t})^2}$, from 1251 to 2019; see section 5.4 and appendix E for details. The shadings around this statistic are 90% Bayesian credible sets. The median 2-, 3-, and 5-year ahead price-level stability statistics are displayed in the top right, bottom left, and bottom right panels along with shadings that are 68% Bayesian credible sets. The price-level stability statistics are computed using the posterior distribution of the TVP-SV-HS-AR(6).

Figure B16: UK Nominal and Real Short- and Long-Term Interest Rates



Notes: The top row plots UK nominal short- and long-term interest rates; see section 6 for details. The bottom row depicts ex ante short- and long-term real rates, $r_{NS,i,t} = R_{BofE,i,t} - E_t \pi_{uk,t+1}$, in the left and right panels, where $i = S$ (short) and L (long). The $r_{NS,S,t}$ ($r_{NS,L,t}$) begins in 1695 (1703) and ends in 2019. One-year ahead expected inflation is computed using the posterior distribution of the TVP-SV-HS-AR(6). In the bottom row of panels, the shadings are 90% Bayesian credible sets.

Appendix C: A MH in Gibbs MCMC Sampler

This section discusses the MH in Gibbs MCMC sampler that draws from the posterior of the baseline iid measurement error model combined with the AR(n) with TVPs and an innovation subject to SV of true inflation, π_t . We reproduce the baseline measurement error model, its state variables, π_t and measurement error, m_t , and the AR(n) with its TVPs and SV as state variables here:

$$\pi_{uk,t} = \pi_t + m_t, \quad (1)$$

$$m_t = \sqrt{\beta_\tau} u_t, \quad u_t \sim \mathcal{N}(0, 1), \quad (2)$$

$$\pi_t = \alpha_{0,t} + \sum_{i=1}^n \alpha_{i,t} \pi_{t-i} + \xi_t \epsilon_t, \quad \epsilon_t \sim \mathcal{N}(0, 1), \quad (3)$$

$$\ln \xi_t^2 = \ln \xi_{t-1}^2 + \sigma_\phi \phi_t, \quad \phi_t \sim \mathcal{N}(0, 1), \quad (4)$$

$$\alpha_t = \alpha_{t-1} + \eta_t, \quad \eta_t \sim \mathcal{N}(0_{n+1}, \Omega_\eta), \quad (5)$$

where $\tau = 1, 2, 3$, and 4 and u_t is uncorrelated with ϵ_t , ϕ_t , and η_t at all leads and lags.

Equation (1) decomposes UK inflation, $\pi_{uk,t}$, into π_t , and m_t . The former is generated by the TVP-SV-AR(n) of equations (3)–(5). Measurement error is iid because it is the realization of the Gaussian innovation u_t scaled by the square root of $\beta_\tau = [1 \ \beta_2 \ \beta_3 \ 0]'$.

The AR(n) of equation (3) is linear in the time-varying intercept, $\alpha_{0,t}$, and lag coefficients, $\alpha_{1,t}, \dots, \alpha_{n,t}$, but nonlinear in the Gaussian innovation ϵ_t that is hit by SV in the form of ξ_t . The log of its square evolves as the geometric random walk (4) in the innovation ϕ_t that is scaled by the static volatility σ_ϕ . Equation (5) is the multivariate random walk generating updates of the time-varying intercept, $\alpha_{0,t}$, and lag coefficients $\alpha_{i,t}$, where $\alpha_t \equiv [\alpha_{0,t} \ \alpha_{1,t} \ \alpha_{2,t} \ \dots \ \alpha_{n,t}]'$ and $\eta_t \equiv [\eta_{0,t} \ \eta_{1,t} \ \eta_{2,t} \ \dots \ \eta_{n,t}]'$. Since the covariance matrix Ω_η is unrestricted, the multivariate random walk (4) yields TVPs that can be correlated. This is not true of the elements of η_t and ϵ_t and ϕ_t because $E(\eta_{i,t} \phi_t) = E(\eta_{i,t} \epsilon_t) = 0$, $i = 0, 1, \dots, n$. A similar restriction is imposed on ϕ_t and ϵ_t , $E(\phi_t \epsilon_t) = 0$.

The MCMC sampler tacks a multivariate random walk proposal-MH decision criterion-robust adaptive Metropolis (RAM) algorithm onto a sequence of Gibbs steps. The MH part draw the three measurement error parameters computing updates using the RAM algorithm of Vihola (2012). The TVPs and SV are drawn in a sequence of Gibbs steps.

The Gibbs component of the MCMC sampler rests on the Canova and Pérez Forero (2015) implementation of the Del Negro and Primiceri (2015) algorithm. This algorithm constructs the posterior of a state space model with SV in the observation equations. Canova and Pérez Forero (2015) apply the algorithm to sample from the posterior of a non-recursive structural VAR with TVPs and SV. We modify instructions in Canova and Pérez Forero (2015) to sample from the TVP-SV-AR(n) of equations (3), (4), and (5). The TVP-SV-AR(n) can be cast as a state space model in which observations on $\pi_{uk,t}$ are connected to the TVPs and SV through equation (3) and these states are generated by the random walks of equations (4) and (5). Our Gibbs MCMC sampler exploits this state space representation to draw from the posterior of α_t and Ω_η similar to the way Canova and Pérez Forero (2015) build on the insights of Carter and Kohn (1994) for Gibbs sampling and algorithm 14 of Chib (2001) to Kalman filter and Kalman smooth the states. Similar Kalman filtering and smoothing routines are employed to make posterior draws of $\ln \xi_t^2$ and σ_ϕ^2 after determining the volatility state \mathbf{s}_t . Drawing \mathbf{s}_t depends on results in Harvey, Ruiz, and Shephard (1994) and Omori, Chib, Shephard, and Nakajima (2007).

A brief sketch of our changes to the Gibbs sampler of Canova and Pérez Forero (2015) clarifies the conditioning needed to draw from the posterior of the TVP-SV-AR(n). Begin by drawing α^T conditional on the current draws of Ω_η , \mathcal{S}^T , ξ^T , σ_ϕ^2 , π^T , and m^T , where, for example, $\mathcal{S}^T = [\mathbf{s}_1 \ \mathbf{s}_2 \ \dots \ \mathbf{s}_t \ \dots \ \mathbf{s}_T]'$. As in Canova and Pérez Forero (2015), we adopt the advice of Koop and Potter (2011) to test whether any α_t in $\alpha^T = [\alpha_1 \ \alpha_2 \ \dots \ \alpha_t \ \dots \ \alpha_T]'$ is explosive by calculating the eigenvalues of the companion matrix:

$$\mathcal{A}_t \equiv \begin{bmatrix} \alpha_{1,t} & \alpha_{2,t} & \dots & \alpha_{n-1,t} & \alpha_{n,t} \\ 1 & 0 & \dots & 0 & 0 \\ 0 & 1 & \dots & 0 & 0 \\ \vdots & \vdots & \ddots & \vdots & \vdots \\ 0 & 0 & \dots & 1 & 0 \end{bmatrix}.$$

If the largest modulus is greater than or equal to one, the proposed draw of α^T is tossed out

and the sampler adds another instance of the previous draw to the posterior. Otherwise, the proposed α^T is retained as the new draw. In either case, the draw helps to update Ω_η , given current draws of \mathcal{S}^T , ξ^T , σ_ϕ^2 , and π^T . Note that a non-diagonal Ω_η is consistent with the multi-move sampler of Carter and Kohn (1994). Next, \mathcal{S}^T is drawn, given updates of α^T and Ω_η and current draws of ξ^T , σ_ϕ^2 , and π^T . This is followed by drawing ξ^T conditional on updates of α^T , Ω_η , and \mathcal{S}^T , and current draws of σ_ϕ^2 and π^T . Finally, draw σ_ϕ^2 conditional on updates of α^T , Ω_η , \mathcal{S}^T , and ξ^T and the current draw of π^T .

Drawing β_2 , β_3 , and the variance of u_t , σ_u^2 , is the MH part of the MCMC sampler. Conditioning on updates of α^T , Ω_η , \mathcal{S}^T , ξ^T , and σ_ϕ^2 and the current draw of π^T , we draw a proposal of $\Psi = [\beta_2 \ \beta_3 \ \sigma_u^2]'$ from a multivariate random walk. The predictive likelihood of the baseline model of equations (1)–(5) is computed using the Kalman filter and updates of the TVPs and SV. The MH criterion is the rule on which the decision is made to accept the proposal of Ψ or hold to the current draw. The RAM computations designed by Vihola (2012) are employed to update the covariance matrix of Φ . Given all the updated draws, the Kalman filter and smoother produce new draws of π^T and m^T .

The MH in Gibbs MCMC algorithm begins step q with the previous posterior draws, $\vec{\alpha}_{q-1}^T$, $\vec{\Omega}_{\eta,q-1}$, $\vec{\mathcal{S}}_{q-1}^T$, $\vec{\xi}_{q-1}^{2T}$, $\vec{\sigma}_{\phi,q-1}^2$, $\vec{\Psi}_{q-1}$, and $\vec{\pi}_{q-1}^T$ and \mathbf{c} , which is a count of the number of times the proposal Ψ has been accepted in the MH step. The following (pseudo) code outlines the algorithm that is conditioned on this information.

- 1) Run the Kalman filter to create $\{\alpha_{t|t}\}_{t=1}^T$ and its mean square error (MSE), $\{\Gamma_{\alpha,t|t}\}_{t=1}^T$, given the initial condition $\alpha_{0|0}$ that is drawn according to the prior listed in Table 2.
 - a) Draw $\check{\alpha}_{T|T} \sim \mathcal{N}(\alpha_{T|T}, \Gamma_{\alpha,T|T})$, which input into the Kalman smoother aids in producing $\check{\alpha}_{T-1|T} \sim \mathcal{N}(\bar{\alpha}_{T-1|T}, \bar{\Gamma}_{\alpha,T-1|T})$, and continue iterating the Kalman smoother backwards in time to obtain smoothed candidate draws $\check{\alpha}^T = \{\check{\alpha}_{t|T}\}_{t=1}^T$, where $\bar{\alpha}_{t|T}$ and its MSE, $\bar{\Gamma}_{\alpha,t|T}$, are outputs of Kalman smoothing operations.
 - b) Employ $\check{\alpha}^T$ to form $\check{\mathcal{A}}^T$. If any $\text{mod}(\check{\mathcal{A}}_t) \geq 1$, discard $\check{\alpha}^T$ and use the previous draw $\vec{\alpha}_{q-1}^T$. Otherwise, update the posterior to $\vec{\alpha}_q^T = \check{\alpha}^T$.
 - c) Compute the empirical moment matrix of $\vec{\alpha}_q^T$, $\Delta_{\alpha,q}$, to draw the update of Ω_η , which is $\vec{\Omega}_{\eta,q} \sim \mathcal{IW}(\underline{\Omega}_\alpha + \Delta_{\alpha,q}, T + n + 1)$.

2) Draw \mathbf{s}_t from the 10-component mixture of Omori, Chib, Shephard, and Nakajima (2007) using the fact ϵ_t is Gaussian.

- a) Given $\vec{\mathcal{S}}^T = \{\vec{\mathbf{s}}_t\}_{t=1}^T$, draw the initial condition $\ln \xi_{0|0}^2$ using the prior in Table 2 to generate $\left\{ \ln \xi_{t|t}^2 \right\}_{t=1}^T$ and its MSE, $\{\gamma_{\xi,t|t}\}_{t=1}^T$, by running the Kalman filter.
- b) Operating the Kalman smoother backwards from date T creates $\vec{\xi}^T = \left\{ \ln \xi_{t|T}^2 \right\}_{t=1}^T$ by first drawing $\ln \xi_{T|T}^2 \sim \mathcal{N}\left(\ln \xi_{T|T}^2, \gamma_{\xi,T|T}\right)$ that in turn helps to produce $\ln \xi_{t|T}^2$ and $\bar{\gamma}_{\xi,t|T}$ to sample $\ln \xi_{t|T}^2 \sim \mathcal{N}\left(\ln \xi_{t|T}^2, \bar{\gamma}_{\xi,t|T}\right)$, $t = T-1, \dots, 1$.
- c) Draw $\vec{\sigma}_{\phi,q}^2 \sim \mathcal{IG}\left(0.5(\nu + T), 0.5(\varsigma + \sigma_{\phi,q}^2)\right)$, where ν and ς are the degrees of freedom and variance of the prior on σ_{ϕ}^2 described in Table 2 and $\sigma_{\phi,q}^2$ is the empirical moment (i.e., sum of squares) of $\vec{\xi}^T$.

3) Generate the proposal $\check{\Upsilon}_q = \check{\Upsilon}_{q-1} + \Omega_{\Upsilon}^{0.5} \varphi$, where $\varphi \sim \mathcal{N}(\mathbf{0}_{3 \times 1}, I_3)$, Ω_{Υ} is the covariance matrix of Υ , $\Omega_{\Upsilon}^{0.5}$ is its Cholesky decomposition, and the vector Υ contains transformations of the elements of Ψ that map from the unit interval to the unbounded real line for $\beta_{2,u}$ and $\beta_{3,u}$, $\Upsilon_1 = \ln \Psi_1 - \ln(1 - \Psi_1)$, $\Upsilon_2 = \ln \Psi_2 - \ln(1 - \Psi_2)$, and from the positive part of the real line to the unbounded real line for σ_u^2 , $\Upsilon_3 = \ln \Psi_3$.

- a) The Kalman filter yields proposals of $\check{\pi}^T$ and \check{m}^T , given $\vec{\alpha}_q^T$, $\vec{\Omega}_{\eta,q}$, $\vec{\xi}_q^{2T}$, $\vec{\sigma}_{\phi,q}^2$, and $\check{\Psi}_q$, along with the predictive likelihood $\mathcal{L}\left(\pi_{uk,t}^T | \vec{\alpha}_q^T, \vec{\Omega}_{\eta,q}, \vec{\xi}_q^{2T}, \vec{\sigma}_{\phi,q}^2, \check{\Psi}_q\right)$
- b) that is an input into the MH criterion

$$\varpi_q = \min \left\{ \frac{\mathcal{L}\left(\pi_{uk,t}^T | \vec{\alpha}_q^T, \vec{\Omega}_{\eta,q}, \vec{\xi}_q^{2T}, \vec{\sigma}_{\phi,q}^2, \check{\Psi}_q\right) g\left(\check{\Psi}_{q-1}, \check{\Psi}_q\right) \mathcal{P}\left(\check{\Psi}_q\right)}{\mathcal{L}\left(\pi_{uk,t}^T | \vec{\alpha}_q^T, \vec{\Omega}_{\eta,q}, \vec{\xi}_q^{2T}, \vec{\sigma}_{\phi,q}^2, \check{\Psi}_{q-1}\right) g\left(\check{\Psi}_q, \check{\Psi}_{q-1}\right) \mathcal{P}\left(\check{\Psi}_{q-1}\right)}, 1 \right\},$$

against a uniform random variable $\omega_q \sim \mathcal{U}(0, 1)$, where $g(\cdot, \cdot)$ is the kernel of the proposal distribution, which is the gradient of the target restricted by its support as discussed by Lindström (2017), and $\mathcal{P}(\cdot)$ is the prior of Ψ .

- c) If $\omega_q \leq \varpi_q$, we have $\vec{\Psi}_q = \check{\Psi}_q$. Otherwise, $\vec{\Psi}_q = \vec{\Psi}_{q-1}$. The latter decision keeps \mathbf{c} unchanged while the former outcome updates $\mathbf{c} = \mathbf{c} + 1$.
- d) Given $\vec{\alpha}_q^T$, $\vec{\Omega}_{\eta,q}$, $\vec{\xi}_q^{2T}$, $\vec{\sigma}_{\phi,q}^2$, and $\vec{\Psi}_q$, the Kalman filter and smoother produce $\vec{\pi}_q^T$ and \vec{m}_q^T .

e) The RAM law of motion of the covariance matrix of Ψ is

$$\Omega_{\Upsilon,q} = \Omega_{\Upsilon,q-1}^{0.5} \Omega_{\Upsilon,q-1}^{0.5'} + \Omega_{\Upsilon,q-1}^{0.5} \left(\min(1, \dim(\Psi) q^\zeta) \times (\omega_q - \omega^*) \frac{\varphi_q \varphi_q'}{\|\varphi_q\|^2} \right) \Omega_{\Upsilon,q-1}^{0.5'}$$

where $\dim(\Psi) = 3$ and ζ is the step size to adapt new proposals. Vihola (2012) suggests $\zeta \approx -0.65$. We set $\omega^* = 0.315$, which is about half way between the optimal acceptance rate for a single parameter model and the optimal acceptance rate of a model with six or more parameters.

4) Repeat steps 1 to 3 to obtain \mathcal{Q} draws, where $q = 1, \dots, \mathcal{Q}$.

Additional information is needed to construct the posterior of a TVP-SV-AR(n) by running the Gibbs component of the MCMC sampler. The Gibbs MCMC sampler calibrates κ_n to yield an acceptance rate for $\{\vec{\alpha}_q^T\}_{q=1}^{\mathcal{Q}}$ ranging from 50% to 60%. The second columns of Tables C1 to C4 lists the values of the tuning parameter, κ_n , that achieves the desired acceptance rate for the baseline model of iid measurement error, the alternative model of iid measurement error, the TVP-SV-AR(n) lacking measurement error, and the same model that invokes the horseshoe prior on SV. The calibrations of κ_n are of note in two ways. First, this tuning parameter is smaller as the lag length n increases in all four tables. Second, κ_n is larger n by n in the models with measurement errors compared with the same columns in Tables C3 and C4.

Next, sampling $\vec{\mathcal{S}}^T$ and $\vec{\xi}^T$ relies on an approximation. Rewrite the TVP-SV-AR(n) as $\vec{\mathcal{Y}}_t \equiv \pi_t - \vec{\alpha}_{0,t} - \sum_{i=1}^k \vec{\alpha}_{i,t} \pi_{t-i} = \xi_t \epsilon_t$, pass the natural log operator through to obtain $\ln \vec{\mathcal{Y}}_t^2 = 2 \ln \xi_t + \ln \epsilon_t^2$, and the approximation $\ln(\vec{\mathcal{Y}}_t^2 + \iota) \approx 2 \ln \xi_t + \ln \epsilon_t^2$, where $\iota = 0.0001$ bounds away from zero the term inside the log on the left of the approximation. Harvey, Ruiz, and Shephard (1994) brought attention to the fact that the log of the square of a Gaussian random deviate is distributed $\ln \epsilon_t^2 \sim \ln \chi^2(1)$ with a mean of -1.2704 and a variance equal to $3.1416^2/2$. Omori, Chib, Shephard, and Nakajima (2007) approximate $\ln \chi^2(1)$ using these facts and a 10-component mixture of normal distributions, which is our source for drawing $\vec{\mathcal{S}}^T$.

The initial condition $\Omega_{\Upsilon,0}$ is drawn from a prior grounded in the \mathcal{IW} distribution. We

endow $\Omega_{\Upsilon,0} \sim \mathcal{IW}\left(T + \dim(\Psi) + 2, 0.001I_{\dim(\Psi)}\right)$. However, β_2 , β_3 , and σ_u^2 are given initial conditions of two-thirds, one-third, and 0.21114^2 , respectively.

The three other models alternative fit easily into the MCMC sampling algorithm summarized by steps 1, 2, and 3. The posterior of the alternative model of iid measurement error is generated as outlined previously except that Ψ is changed to $[\sigma_{1,u}^2 \ \sigma_{2,u}^2 \ \sigma_{3,u}^2]'$. Table B1 presents the priors of the three measurement error parameters of the alternative model. Results for this model are reported in Appendix B.2. The algorithm is a pure Gibbs MCMC sampler for the two models lacking measurement error because step 3 is dropped. The TVP-SV-AR(n) with the horseshoe prior is reviewed in Appendix B.4 while the standard specification of SV is discussed in Appendix B.3.

We generate a burn-in of $0.5Q = 250,000$ steps from the MH in Gibbs MCMC sampler and create Q posterior draws. Results are reported for the four models on a thinned posterior. The Q posterior draws are thinned using random sampling without replacement of the integers $q = 1, \dots, Q$. The thinned posteriors consist of $\mathcal{D} = 2000$ draws.

The right most column of Tables C1 to C4 report the run-times of the four models. Not surprisingly, the models setting $\pi_{uk,t} = \pi_t$ have shorter run-times compared with the baseline and alternative iid measurement error models. The horseshoe prior adds marginally to the run-time relative to the model of equations (3)–(5). The baseline and alternative iid measurement error models can take from about two and quarter hours at $n = 1$ to a run-time between 10 and 11 hours for $n = 6$. The run-time of the models lacking measurement error is 210 minutes or less.

The MH in Gibbs MCMC and Gibbs MCMC samplers are run using `Julia v.1.6.6`. The same statistical and computational software is employed to calculate the log MDDs, the WAICs, and the R_{ht}^2 and price stability statistics. The Estima econometric software package RATS is the source of the unit root tests in Table 1 and the MA and Newey-West confidence bands displayed in Figure 2. The remaining figures are constructed using the `Julia` packages `PyPlot` and `PyCall` to engage the `Python` package `Matplotlib v3.4.2`.

**Table C1. Summary of the MH in Gibbs MCMC Sampler for the TVP-SV-AR(n)
with Baseline Model of iid Measurement Error**

n	κ_η	Stationary Acceptance Rate $\{\alpha_q^T\}_{q=1}^Q$	Elapsed Run-Time
1	98.50	52.5%	2.25 hours
2	28.50	52.5%	3.37 hours
3	7.75	55.1%	4.40 hours
4	4.75	55.1%	6.32 hours
5	3.25	53.2%	8.47 hours
6	2.38	52.3%	10.90 hours

Notes: The second column of the table reports the tuning parameter, κ_η , on the prior of the initial covariance matrix of the intercept and lag coefficients, α_t , the acceptance rate of the stationary lag TVPs, $\alpha_{\ell,t}$, $\ell = 1, \dots, n$, and the speed in (real) time needed to run the MH in Gibbs MCMC sampler on equations (1)–(5) of the paper and the long annual UK inflation sample.

**Table C2. Summary of the MH in Gibbs MCMC Sampler for the TVP-SV-AR(n)
with Alternative Model of iid Measurement Error**

n	κ_η	Stationary Acceptance Rate $\{\alpha_q^T\}_{q=1}^Q$	Elapsed Run-Time
1	108.50	52.8%	2.27 hours
2	33.50	53.0%	3.30 hours
3	7.98	55.4%	4.38 hours
4	5.85	53.0%	6.52 hours
5	3.95	52.4%	8.58 hours
6	3.18	52.4%	10.48 hours

Notes: See the notes to Table C1, but the speed in (real) time needed to run the MH in Gibbs MCMC sampler is on equation (1) and equations (3)–(5) of the paper, $m_t = \sigma_{\tau,u} u_t$, and the long annual UK inflation sample, where $\tau = 1, 2$, and 3.

Table C3. Summary of the Gibbs MCMC Sampler for the TVP-SV-AR(n)

n	κ_η	Stationary Acceptance Rate $\{\alpha_q^T\}_{q=1}^Q$	Elapsed Run-Time
1	88.50	58.4%	0.42 hours
2	77.50	52.8%	1.00 hours
3	7.28	53.5%	1.33 hours
4	3.50	57.3%	2.00 hours
5	2.18×10^{-1}	57.1%	2.47 hours
6	1.50×10^{-1}	51.2%	3.33 hours

Notes: See the notes to Table C1, but elapsed run-time is the speed in (real) time needed to run the Gibbs MCMC sampler on the TVP-SV-AR(n)s and long annual UK inflation sample, where $\pi_{uk,t} = \pi_t$.

Table C4. Summary of the Gibbs MCMC Sampler for the TVP-SV-AR⁽ⁿ⁾ with the Horseshoe Prior on SV

n	κ_η	Stationary Acceptance Rate $\{\alpha_q^T\}_{q=1}^Q$	Elapsed Run-Time
1	90.80	53.0%	0.58 hours
2	73.80	58.0%	1.07 hours
3	7.98	51.1%	1.48 hours
4	2.38	57.7%	1.87 hours
5	2.12×10^{-1}	52.2%	2.75 hours
6	1.25×10^{-1}	58.8%	3.35 hours

Notes: See the notes to Table C3.

Appendix D: The Formula for Inflation Predictability

We use the R^2 statistic proposed by Cogley, Primiceri, and Sargent (2010) to summarize the h -year ahead predictability of UK inflation, $\pi_{uk,t}$. The R^2 statistic is one minus the ratio of the conditional variance to the unconditional variance. It lies between 0 and 1. If the series is completely unpredictable, the conditional variance and unconditional variances coincide forcing the ratio to unity and $R^2 = 0$. Also, it goes to zero as $h \rightarrow \infty$.

Computing the R^2 statistic relies on the TVP-SV-AR(n) with measurement error be in companion form. Recall that ξ_t is the date- t , scalar SV of the AR(n) and $\beta_\tau \sigma_u u_t$ is measurement error. Define $\Pi_{uk,t} \equiv [\pi_{uk,t} \ \pi_{uk,t-1} \ \dots \ \pi_{uk,t-n+1}]'$, $\mathcal{A}_{0,t} \equiv [\alpha_{0,t} \ 0 \ \dots \ 0]'$, $\Pi_t \equiv [\pi_t \ \pi_{t-1} \ \dots \ \pi_{t-n+1}]'$, $\mathcal{M}_t \equiv [m_t \ m_{t-1} \ \dots \ m_{t-n+1}]'$, $m_t = \sqrt{\beta_\tau} \sigma_u u_t$, $\Xi_t \equiv [\xi_t \epsilon_t \ 0 \ \dots \ 0]'$, and remember Appendix C defines the date t companion matrix of the AR(n) as:

$$\mathcal{A}_t \equiv \begin{bmatrix} \alpha_{1,t} & \alpha_{2,t} & \dots & \alpha_{n-1,t} & \alpha_{n,t} \\ 1 & 0 & \dots & 0 & 0 \\ 0 & 1 & \dots & 0 & 0 \\ \vdots & \vdots & \ddots & \vdots & \vdots \\ 0 & 0 & \dots & 1 & 0 \end{bmatrix}.$$

Putting the definitions together let us write the TVP-SV-AR(n) in companion form as:

$$\Pi_{uk,t} = \mathcal{A}_{0,t} + \mathcal{A}_t \Pi_{t-1} + \mathcal{N} \mathcal{M}_t + \Xi_t, \quad (D1)$$

where \mathcal{N} is a $n \times n$ matrix full of zeros except for a one as the first diagonal element.

Cogley, Primiceri, and Sargent (2010) invoke the anticipated utility model (AUM) of Kreps (1998) as implemented by Cogley and Sbordone (1998) to calculate the R^2 statistic. This version of the AUM assumes a local approximation that holds posterior draws of $\mathcal{A}_{0,t+j}$ and \mathcal{A}_{t+j} at their current realizations to forecast inflation j -years ahead, $E_t \pi_{t+j}$.

This assumption yields the statistic:

$$R_{ht}^2 \approx 1 - \frac{s_1 \left[\sum_{j=0}^{h-1} \mathcal{A}_t^j \Omega_{u,\Xi,t} \left(\mathcal{A}_t^j \right)' \right] s_1'}{s_1 \left[\sum_{j=0}^{\infty} \mathcal{A}_t^j \Omega_{u,\Xi,t} \left(\mathcal{A}_t^j \right)' \right] s_1'}, \quad (D2)$$

which measures the total predictability of $\pi_{uk,t}$ at horizon h and year t with respect to true inflation, π_t , and measurement error, $\sqrt{\beta_\tau} \sigma_u u_t$, where the selection vector $s_1 = [1 \ 0 \ \dots \ 0]_{1 \times n}$, $\Omega_{u,\Xi,t} = \mathcal{A}_t \Omega_{u,t} \mathcal{A}_t' + \mathcal{N} \Omega_{u,t} \mathcal{N}' + \Omega_{\Xi,t}$, $\Omega_{u,t} = \mathcal{M}_t \mathcal{M}_t'$, and $\Omega_{\Xi,t} = \Xi_t \Xi_t'$.

Pass the *vec* operator through the $n \times n$ matrix $\sum_{j=0}^{\infty} \mathcal{A}_t^j \Omega_{u,\Xi,t} (\mathcal{A}_t^j)'$ in the denominator of (D2) and employ the rule of vectorizing three conformable matrices to find $[I_{n^2} - (\mathcal{A}_t \otimes \mathcal{A}_t)]^{-1} \left[[\mathcal{A}_t \otimes \mathcal{A}_t + \mathcal{N} \otimes \mathcal{N}] \text{vec}(\Omega_{u,t}) + \text{vec}(\Omega_{\Xi,t}) \right]$, which is a n^2 column vector. This lets us define the initial infinite sum as the $n \times n$ matrix:

$$\mathcal{A}_{\infty,t} = \text{reshape} \left([I_{n^2} - (\mathcal{A}_t \otimes \mathcal{A}_t)]^{-1} \left[[\mathcal{A}_t \otimes \mathcal{A}_t + \mathcal{N} \otimes \mathcal{N}] \text{vec}(\Omega_{u,t}) + \text{vec}(\Omega_{\Xi,t}) \right], n, n \right).$$

In the numerator, adding and subtracting $\sum_{j=h}^{\infty} \mathcal{A}_t^j \Omega_{u,\Xi,t} (\mathcal{A}_t^j)'$ equates the finite sum $\sum_{j=0}^{h-1} \mathcal{A}_t^j \Omega_{u,\Xi,t} (\mathcal{A}_t^j)'$ to $\sum_{j=0}^{\infty} \mathcal{A}_t^j \Omega_{u,\Xi,t} (\mathcal{A}_t^j)'$ - $\sum_{j=h}^{\infty} \mathcal{A}_t^j \Omega_{u,\Xi,t} (\mathcal{A}_t^j)'$. The change of index $j = \ell + h$ yields:

$$\sum_{j=h}^{\infty} \mathcal{A}_t^j \Omega_{u,\Xi,t} (\mathcal{A}_t^j)' = \sum_{\ell=0}^{\infty} \mathcal{A}_t^{\ell+h} \Omega_{u,\Xi,t} (\mathcal{A}_t^{\ell+h})' = \mathcal{A}_t^h \left[\sum_{\ell=0}^{\infty} \mathcal{A}_t^{\ell} \Omega_{u,\Xi,t} (\mathcal{A}_t^{\ell})' \right] (\mathcal{A}_t^h)'$$

Combining the last two equations produces:

$$\sum_{j=0}^{\infty} \mathcal{A}_t^j \Omega_{u,\Xi,t} (\mathcal{A}_t^j)' - \sum_{j=h}^{\infty} \mathcal{A}_t^j \Omega_{u,\Xi,t} (\mathcal{A}_t^j)' = \mathcal{A}_{\infty,t} - \mathcal{A}_t^h \mathcal{A}_{\infty,t} (\mathcal{A}_t^h)',$$

revises equation (D2) as:

$$R_{ht}^2 \approx 1 - \frac{s_1 \left[\mathcal{A}_{\infty,t} - \mathcal{A}_t^h \mathcal{A}_{\infty,t} (\mathcal{A}_t^h)' \right] s_1'}{s_1 \mathcal{A}_{\infty,t} s_1'}. \quad (D3)$$

Equation (D3) measures R_{ht}^2 for the analyst unaware of measurement error in $\pi_{uk,t}$. Nonetheless, R_{ht}^2 can be decomposed into the contributions of innovations to the AR(n), $\xi_t \epsilon_t$, of true inflation, π_t , and of the additive measurement error, $\sqrt{\beta_{\tau}} \sigma_u u_t$. This also omits draws of \mathcal{A}_t , $\Omega_{u,t}$, and $\Omega_{\Xi,t}$ from the posterior of TVP-SV-AR(n).

Our goal is to report the predictability of π_t at horizon h for an economic agent able to observe true inflation. Computing the contribution of Ξ_t for R_{ht}^2 sets to zero the variance of measurement error of the τ th span, $\beta_{\tau} \sigma_u^2$, which is the (1, 1) element of $\Omega_{u,t}$. This restricts $\mathcal{A}_{\infty,t} = \text{reshape} \left([I_{n^2} - (\mathcal{A}_t \otimes \mathcal{A}_t)]^{-1} \text{vec}(\Omega_{\Xi,t}), n, n \right)$ in the numerator and denominator of equation (D3). In other words, for the conditional and unconditional variances we report the contributions of movements in true inflation, π_t , to the h -year ahead predictability of sample inflation, $\pi_{uk,t}$.

Appendix E: The Formula for Price-Level Instability

At horizon h , instability in the UK price level is given by equation (8) of the paper:

$$\sqrt{\text{var}_t(p_{uk,t+h} - E_t p_{uk,t+h}) + (E_t p_{uk,t+h} - p_{uk,t})^2}, \quad (8)$$

which is the square root of a conditional variance plus a squared, conditional mean.

The equation generating the volatility or uncertainty surrounding $E_t p_{uk,t+h} - p_{uk,t}$, similar to equation (9) of Cogley, Sargent, and Surico (2015), is connected to the expected accumulation of inflation over a h -year ahead horizon, $E_t \sum_{j=1}^h \pi_{uk,t+j}$. However, they use a different parametric model of inflation. In our case, the conditional mean of inflation, $E_t p_{uk,t+1} - p_{uk,t} = E_t \pi_{t+1} = s_1 [\tilde{\mathcal{A}}_{0,t} + \tilde{\mathcal{A}}_t \hat{\Pi}_t]$ at $h = 1$ using equations (1), (2), and (3) of the paper, which equate $\pi_{uk,t}$ to the sum of true inflation, π_t , and measurement error, m_t , and are the measurement error process and TVP-SV-AR(n) of true inflation, where $\tilde{\mathcal{A}}_{0,t}$ and $\tilde{\mathcal{A}}_t$ are draws from the posterior distribution of the TVP-SV-AR(n).

For $h \geq 2$, calculating $E_t p_{uk,t+h} - p_{uk,t}$ is more difficult because of the TVPs. First, define $\mathcal{C}_t \equiv (I_n - \mathcal{A}_t)^{-1} \mathcal{A}_{0,t}$ and then substitute for $\mathcal{A}_{0,t}$ in the companion form of the TVP-SV-AR(n) of true inflation, $\Pi_t = \mathcal{A}_{0,t} + \mathcal{A}_t \Pi_{t-1} + \Xi_t$, and rearrange terms:

$$\Pi_t - \mathcal{C}_t = -\mathcal{A}_t (\mathcal{C}_t - \mathcal{C}_{t-1}) + \mathcal{A}_t (\Pi_{t-1} - \mathcal{C}_{t-1}) + \Xi_t.$$

Push this equation h -years ahead and pass through the expectations operator to find:

$$E_t (\pi_{t+h} - c_{t+h}) = s_1 E_t \left(\mathcal{A}_{t+h} \left[(\mathcal{C}_{t+h-1} - \mathcal{C}_{t+h}) + (\Pi_{t+h-1} - \mathcal{C}_{t+h-1}) \right] \right),$$

where $E_t (\pi_{t+h} - c_{t+h}) = s_1 E_t (\Pi_{t+h} - \mathcal{C}_{t+h})$ and disregard differences between $\tilde{\mathcal{A}}_{0,t}$ and $\mathcal{A}_{0,t}$ and $\tilde{\mathcal{A}}_t$ and \mathcal{A}_t until later. Since $E_t (\pi_{t+1} - c_{t+1}) = s_1 \mathcal{A}_t \left[(\mathcal{C}_t - \mathcal{C}_{t+1}) + (\Pi_t - \mathcal{C}_t) \right]$, iterating forward and substituting produces:

$$E_t (\pi_{t+h} - c_{t+h}) = s_1 E_t \left(\sum_{j=1}^h \left(\prod_{\ell=1}^j \mathcal{A}_{t+h+\ell-j} \right) [\mathcal{C}_{t+h-j} - \mathcal{C}_{t+h+\ell-j}] + \prod_{j=1}^h \mathcal{A}_{t+j} [\Pi_t - \mathcal{C}_t] \right).$$

Next, apply the AUM to the previous equation, $E_t \pi_{t+h} = s_1 [\mathcal{C}_t + \mathcal{A}_t^h (\Pi_t - \mathcal{C}_t)]$, and replace \mathcal{C}_t with $(I_n - \mathcal{A}_t)^{-1} \mathcal{A}_{0,t}$ to give $E_t \pi_{uk,t+h} = s_1 \left([I_n - \mathcal{A}_t^h] (I_n - \mathcal{A}_t)^{-1} \mathcal{A}_{0,t} + \mathcal{A}_t^h \Pi_t \right)$,

which when summed from 1- to h -years ahead results in:

$$E_t p_{uk,t+h} - p_{uk,t} = s_1 \left(\left[hI_n - \sum_{j=1}^h \mathcal{A}_t^j \right] (I_n - \mathcal{A}_t)^{-1} \mathcal{A}_{0,t} + \sum_{j=1}^h \mathcal{A}_t^j \Pi_t \right), \quad (E1)$$

where $\mathcal{A}_{0,t}$ and \mathcal{A}_t are held at their current realizations to forecast the sum of inflation h -years ahead, $E_t p_{uk,t+h}$ is conditional on the history of inflation, TVPs, and SV through date t (i.e., $x^t = [x_t \ x_{t-1} \ \dots \ x_1]$, $x^t = \pi^t$, \mathcal{A}^t , and ξ^t) and the (hyper-)parameter σ_ϕ . Given draws from the posterior distribution of a TVP-SV-AR(n), squaring equation (E1) produces $(E_t p_{uk,t+h} - p_{uk,t})^2$.

The conditional variance $(E_t p_{uk,t+h} - p_{uk,t})^2$ is also computed given $\mathcal{A}_{0,t}$ and \mathcal{A}_t are known at year t . Hence,

$$(E_t p_{uk,t+h} - p_{uk,t})^2 = s_1 \left(\sum_{j=1}^h \mathcal{A}_t^j E_t (\Pi_t \Pi_t') \left(\sum_{j=1}^h \mathcal{A}_t^j \right)' \right) s_1'. \quad (E2)$$

The right hand side of equation (3) is evaluated numerically by replacing $\sum_{j=1}^h \mathcal{A}_t^j$ with $\mathcal{A}_t (I_n - \mathcal{A}_t^h) (I_n - \mathcal{A}_t)^{-1}$ and $E_t (\Pi_t \Pi_t') = \Omega_\Pi$ is the unconditional variance of Π_t because $\mathcal{A}_{0,t}$ and \mathcal{A}_t are known at year t , and $\text{vec}(\Omega_\Pi) = [I_{n^2} - \mathcal{A}_t \otimes \mathcal{A}_t]^{-1} \text{vec}(\Omega_{\Xi,t})$ using the companion form of the TVP-SV-AR(n) of true inflation and the rule for vectorizing three conformable matrices.

We calculate the conditional variance, $\text{var}_t(p_{uk,t+h} - E_t p_{uk,t+h})$, recognizing its equivalence to $\text{var}_t(\pi_{uk,t+h} - E_t \pi_{uk,t+h} + p_{uk,t+h-1} - E_t p_{uk,t+h-1})$. Since the innovation to the h -year ahead price level forecast is $p_{uk,t+h} - E_t p_{uk,t+h} = s_1 [\Pi_{uk,t+h} - E_t \Pi_{uk,t+h}] + p_{uk,t+h-1} - E_t p_{uk,t+h-1}$, the first component of this recursion is constructed using the companion form of the TVP-SV-AR(n). This is equation (D1) in the previous section. At $h = 1$, the forecast error of the observed price level is:

$$p_{uk,t+1} - E_t p_{uk,t+1} = s_1 \left[\tilde{\mathcal{A}}_{0,t+1} - \tilde{\mathcal{A}}_{0,t} + (I_n - E_t) \tilde{\mathcal{A}}_{t+1} \hat{\Pi}_t + \mathcal{N} \mathcal{M}_{t+1} + \Xi_{t+1} \right], \quad (E3)$$

where $\hat{\Pi}_t$ contains Kalman smoothed predictions of Π_t . Define $\mathcal{H}_{0,t+1} \equiv [\eta_{0,t+1} \ 0 \ 0 \ \dots \ 0]'$, $\eta_{0,t+1} = s_1 \mathcal{H}_{0,t+1}$, $\sqrt{\beta_\tau} \sigma_u u_{t+1} = s_1 \mathcal{N} \mathcal{M}_{t+1}$, and $\xi_{t+1} \eta_{t+1} = s_1 \Xi_{t+1}$ to turn equation (E3)

into $p_{uk,t+1} - E_t p_{uk,t+1} = \eta_{0,t+1} + s_1 (I_n - E_t) \mathcal{A}_{t+1} \Pi_t + \sqrt{\beta_\tau} \sigma_u u_{t+1} + \xi_{t+1} \eta_{t+1}$, where we continue to ignore differences between $\tilde{\mathcal{A}}_{t+1}$ and \mathcal{A}_{t+1} and $\hat{\Pi}_t$ and Π_t .

For $h \geq 2$, only $\pi_{uk,t+h} - E_t \pi_{uk,t+h}$ is needed to update the forecast error of the price level. Moving from horizon $h = 1$ to $h = 2$ lets us focus on computing:

$$\begin{aligned} \pi_{uk,t+2} - E_t \pi_{uk,t+2} = & s_1 \left[\mathcal{A}_{0,t+2} - \mathcal{A}_{0,t} + (I_n - E_t) \left[\mathcal{A}_{t+2} \mathcal{A}_{0,t+1} + \mathcal{A}_{t+2} \mathcal{A}_{t+1} \Pi_t \right] \right. \\ & \left. + \mathcal{N} \mathcal{M}_{t+2} + \mathcal{A}_{t+2} \mathcal{N} \mathcal{M}_{t+1} + \Xi_{t+2} + \mathcal{A}_{t+2} \Xi_{t+1} \right]. \end{aligned}$$

Combining the last expression with equation (E3) yields:

$$\begin{aligned} p_{uk,t+2} - E_t p_{uk,t+2} = & s_1 \left[\sum_{j=1}^2 (3-j) \mathcal{H}_{0,t+j} + (I_n - E_t) \left[\mathcal{A}_{t+2} \mathcal{A}_{0,t+1} + (\mathcal{A}_{t+2} \mathcal{A}_{t+1} + \mathcal{A}_{t+1}) \Pi_t \right] \right. \\ & \left. + \mathcal{N} \mathcal{M}_{t+2} + (I_n + \mathcal{A}_{t+2}) \mathcal{N} \mathcal{M}_{t+1} + \Xi_{t+2} + (I_n + \mathcal{A}_{t+2}) \Xi_{t+1} \right]. \quad (E4) \end{aligned}$$

Using the same arguments at $h = 3$ gives:

$$\begin{aligned} \pi_{uk,t+3} - E_t \pi_{uk,t+3} = & s_1 \left[\mathcal{A}_{0,t+3} - \mathcal{A}_{0,t} + (I_n - E_t) \left[\mathcal{A}_{t+3} \mathcal{A}_{0,t+2} + \mathcal{A}_{t+3} \mathcal{A}_{t+2} \mathcal{A}_{0,t+1} \right] \right. \\ & + (I_n - E_t) \mathcal{A}_{t+3} \mathcal{A}_{t+2} \mathcal{A}_{t+1} \Pi_t \\ & + \mathcal{N} \mathcal{M}_{t+3} + \mathcal{A}_{t+3} \mathcal{N} \mathcal{M}_{t+2} + \mathcal{A}_{t+3} \mathcal{A}_{t+2} \mathcal{N} \mathcal{M}_{t+1} \\ & \left. + \Xi_{t+3} + \mathcal{A}_{t+3} \Xi_{t+2} + \mathcal{A}_{t+3} \mathcal{A}_{t+2} \Xi_{t+1} \right], \end{aligned}$$

that added to equation (E4) results in:

$$\begin{aligned} p_{uk,t+3} - E_t p_{uk,t+3} = & s_1 \left[\sum_{j=1}^3 (4-j) \mathcal{H}_{0,t+j} + (I_n - E_t) \left(\mathcal{A}_{t+3} \mathcal{A}_{0,t+2} + \mathcal{A}_{t+3} \mathcal{A}_{t+2} \mathcal{A}_{0,t+1} \right. \right. \\ & \left. \left. + \mathcal{A}_{t+2} \mathcal{A}_{0,t+1} + \left[\mathcal{A}_{t+3} \mathcal{A}_{t+2} \mathcal{A}_{t+1} + \mathcal{A}_{t+2} \mathcal{A}_{t+1} + \mathcal{A}_{t+1} \right] \Pi_t \right) \right. \\ & + \mathcal{N} \mathcal{M}_{t+3} + (I_n + \mathcal{A}_{t+3}) \mathcal{N} \mathcal{M}_{t+2} + (I_n + \mathcal{A}_{t+3} \mathcal{A}_{t+2}) \mathcal{N} \mathcal{M}_{t+1} \\ & \left. + \Xi_{t+3} + (I_n + \mathcal{A}_{t+3}) \Xi_{t+2} + (I_n + \mathcal{A}_{t+3} \mathcal{A}_{t+2}) \Xi_{t+1} \right]. \quad (E5) \end{aligned}$$

We infer from equations (E4) and (E5) that the conditional forecast error of the observed price level for $h \geq 2$ is:

$$\begin{aligned}
p_{uk,t+h} - E_t p_{uk,t+h} &= s_1 \left[\sum_{j=1}^h (h+1-j) \mathcal{H}_{0,t+j} + (I_n - E_t) \left[\sum_{j=1}^{h-1} \mathcal{A}_{t+j+1} \mathcal{A}_{0,t+j} \right. \right. \\
&\quad \left. \left. + \prod_{j=1}^{h-1} \mathcal{A}_{t+j+1} \mathcal{A}_{0,t+1} + \sum_{j=1}^h \left(\prod_{\ell=1}^j \mathcal{A}_{t+\ell} \right) \Pi_t \right] + \sum_{j=1}^h (\mathcal{N}\mathcal{M}_{t+j} + \Xi_{t,j}) \right. \\
&\quad \left. + \sum_{j=1}^{h-1} \left(\prod_{\ell=j}^{h-1} \mathcal{A}_{t+\ell+1} \right) [\mathcal{N}\mathcal{M}_{t+j} + \Xi_{t,j}] \right], \tag{E6}
\end{aligned}$$

where $\Xi_{t,j} = [\xi_{t+j} \epsilon_{t+j} \ 0 \ 0 \ \dots \ 0]'$ and $\xi_{t+j} = \xi_t \exp\left(0.5 \sigma_\phi \prod_{i=1}^j \phi_{t+i}\right)$.

The expression on the right of equations (E6) shows the conditional forecast error of $p_{uk,t+h}$ depends on future intercept and lagged TVPs, current true inflation, and future measurement errors and SVs. The latter two elements are summed from 1- to h -years ahead weighted by future realizations of the companion matrix, \mathcal{A}_t , of lagged TVPs. Similarly, current true inflation is discounted by \mathcal{A}_t from 1- to h -years ahead.

Once again, we invoke the local approximation of the AUM to compute the instability statistic using equation (E6). Imposing the AUM on the $\mathcal{A}_{0,t+j}$ s and \mathcal{A}_{t+j} s that appear in equation (E6) creates the local approximation:

$$\begin{aligned}
p_{uk,t+h} - E_t p_{uk,t+h} &\approx s_1 \left[\sum_{j=1}^h (h+1-j) \mathcal{H}_{0,t+j} + \sum_{j=1}^h (\mathcal{N}\mathcal{M}_{t+j} + \Xi_{t,j}) \right. \\
&\quad \left. + \sum_{j=1}^{h-1} \mathcal{A}_t^{h-j} [\mathcal{N}\mathcal{M}_{t+j} + \Xi_{t,j}] \right].
\end{aligned}$$

Since $\text{var}_t(p_{uk,t+h} - E_t p_{uk,t+h}) = E_t \left\{ (p_{uk,t+h} - E_t p_{uk,t+h})^2 \right\}$, multiple the right hand side of the previous equation by its transpose to produce:

$$\begin{aligned}
\text{var}_t(p_{uk,t+h} - E_t p_{uk,t+h}) &\approx E_t \left(s_1 \left[\sum_{j=1}^h (h+1-j) \mathcal{H}_{0,t+j} + \sum_{j=1}^h (\mathcal{N}\mathcal{M}_{t+j} + \Xi_{t,j}) \right. \right. \\
&\quad \left. \left. + \sum_{j=1}^{h-1} \mathcal{A}_t^{h-j} [\mathcal{N}\mathcal{M}_{t+j} + \Xi_{t,j}] \right] \left[\sum_{j=1}^h (h+1-j) \mathcal{H}_{0,t+j} \right. \right. \\
&\quad \left. \left. + \sum_{j=1}^h (\mathcal{N}\mathcal{M}_{t+j} + \Xi_{t,j}) + \sum_{j=1}^{h-1} \mathcal{A}_t^{h-j} [\mathcal{N}\mathcal{M}_{t+j} + \Xi_{t,j}] \right] \right)'. \tag{E7}
\end{aligned}$$

In equation (E7), the summations from $j = 1$ to $h-1$ are only relevant for $h \geq 2$. Performing the arithmetic of equation (E7) leads to:

$$\begin{aligned}
\text{var}_t(p_{uk,t+h} - E_t p_{uk,t+h}) &\approx \sum_{j=1}^h (h+1-j)^2 s_1 E_t \left(\mathcal{H}_{0,t+j} \mathcal{H}'_{0,t+j} \right) s'_1 \\
&+ s_1 \mathcal{N} \sum_{j=1}^h E_t \left(\mathcal{M}_{t+j} \mathcal{M}'_{t+j} \right) \mathcal{N}' s'_1 + s_1 \sum_{j=1}^h E_t \left(\Xi_{t,j} \Xi'_{t,j} \right) s'_1 \\
&+ s_1 \sum_{j=1}^{h-1} \mathcal{A}_t^{h-j} \left[\mathcal{N} E_t \left(\mathcal{M}_{t+j} \mathcal{M}'_{t+j} \right) \mathcal{N}' \right] \left(\mathcal{A}_t^{h-j} \right)' s'_1 \\
&+ s_1 \sum_{j=1}^{h-1} \mathcal{A}_t^{h-j} \left[E_t \left(\Xi_{t,j} \Xi'_{t,j} \right) \right] \left(\mathcal{A}_t^{h-j} \right)' s'_1 \\
&= \left[\frac{h(h+1)(2h+1)}{6} \right] \sigma_{\eta,0}^2 + h\sigma_{m,\tau}^2 + \underline{\sigma}_{\xi,h,t}^2 \\
&+ s_1 \sum_{j=1}^{h-1} \mathcal{A}_t^{h-j} \left[\mathcal{N} \Omega_{m,\tau,j} \mathcal{N}' + \Omega_{\Xi,t,j} \right] \left(\mathcal{A}_t^{h-j} \right)' s'_1, \quad (E8)
\end{aligned}$$

where $E_t(\epsilon_{t+h}\epsilon_{t+j}) = E_t(u_{t+h}u_{t+j}) = 0$ for $h \neq j$, u_t , and ϵ_t are uncorrelated at all leads and lags, along with being uncorrelated with Π_t , \mathcal{A}_t is in the date t information set, $E_t(\mathcal{H}_{0,t+j}\mathcal{H}'_{0,t+j})$ is a $n \times n$ matrix with $\sigma_{\eta,0}^2$ in its $(1,1)$ position and zeros everywhere else, $\Omega_{m,\tau} = E_t(\mathcal{M}_{t+j}\mathcal{M}'_{t+j})$ is a $n \times n$ matrix full of zeros, but its $(1,1)$ element is $\sigma_{m,\tau}^2$, which is $\beta_\tau \sigma_u^2$, and $\Omega_{\Xi,t} = E_t(\Xi_{t,j}\Xi'_{t,j})$ is a $n \times n$ matrix of zeros except its $(1,1)$ element is $\underline{\sigma}_{\xi,j,t}^2 = E_t \xi_{t+j}^2 = \xi_t^2 E_t \exp(\sigma_\phi \sum_{i=1}^j \phi_{t+i}) = \xi_t^2 \exp(\frac{j}{2} \sigma_\phi^2)$ because ϕ_t is distributed standard normal. Lastly, the term attached to $\sigma_{\eta,0}^2$ is calculated recognizing $\sum_{j=1}^h (h+1-j)^2 = h(h+1)^2 - 2(h+1) \sum_{j=1}^h j + \sum_{j=1}^h j^2$. Since $\sum_{i=j}^h j = 0.5h(h+1)$ and $\sum_{j=1}^h j^2 = h(h+1)(2h+1)/6$, $\sum_{i=0}^h (h+1-j)^2 = h(h+1)(2h+1)/6$. The result is $h(h+1)(2h+1)/6$, which equals 1, 5, 14, and 55 at $h = 1, 2, 3$, and 5.

Equation (E8) shows the effect of using a TVP-SV-AR(n) with measurement error to generate price-level uncertainty, $\text{var}_t(p_{uk,t+h} - E_t p_{uk,t+h})$. Price-level uncertainty is driven by the variances of measurement error and SV of the TVP-SV-AR(n). The impact

of the sums of the measurement error variance and SV on the uncertainty surrounding the price-level depend on the persistence embedded in \mathcal{A}_t .

Instability in the UK price level is calculated by summing the square root of the sum of price-level uncertainty, $\text{var}_t(p_{uk,t+h} - E_t p_{uk,t+h})$, and the uncertainty surrounding $E_t p_{uk,t+h} - p_{uk,t}$. This is equation (8) of the paper. The former conditional variance is computed, as noted in the previous paragraph, using equation (E8) that shows the impact of the scale volatility on the innovation to the random walk of the TVP intercept, measurement error, SV, and lagged TVPs on the instability of $p_{uk,t}$ at forecast horizon h . Similarly, equation (E2) measures the contribution of the uncertainty surrounding $E_t p_{uk,t+h} - p_{uk,t}$ to instability in $p_{uk,t}$ but only with SV and the lagged TVPs. Lastly, we calculate these conditional variances on the posterior distributions of the TVP-SV-AR(n)s with and without measurement error.

References

- Allen, R. C., “The Great Divergence in European Wages and Prices from the Middle Ages to the First World War,” *Explorations in Economic History* 38 (2001), 411–447.
- Amir-Ahmadi, P., C. Matthes and M-C. Wang, “Drifts and Volatilities under Measurement Error: Assessing Monetary Policy Shocks over the Last Century,” *Quantitative Economics* 7 (2016), 591–611.
- Bitto, A. and S. Frühwirth-Schnatter, “Achieving Shrinkage in a Time-varying Parameter Model Framework,” *Journal of Econometrics* 210 (2019), 75–97.
- Cadonna, A., S. Frühwirth-Schnatter and P. Knaus, “Triple the Gamma: A Unifying Shrinkage Prior for Variance and Variable Selection in Sparse State Space and TVP Models,” *Econometrics* 8 (2020), 20.
- Canova, F. and F. J. Pérez Forero, “Estimating overidentified, Nonrecursive, Time-varying Coefficients Structural Vector Autoregressions,” *Quantitative Economics* 6 (2015), 359–384.
- Carter, C. K. and R. Kohn, “On Gibbs Sampling for State Space Models,” *Biometrika* 81 (1994), 541–553.
- Carvalho, C. M., N. G. Polson and J. G. Scott, “The Horseshoe Estimator for Sparse Signals,” *Biometrika* 97 (2010), 465–480.
- Chib, S., “Markov Chain Monte Carlo Methods: Computation and Inference,” in J. J. Heckman and E. Leamer, eds., *Handbook of Econometrics*, vol. 5 (New York: Elsevier Science B.V., 2001) 3569–3649.
- Crafts, N. F. R. and T. C. Mills, “Trends in Real Wages in Britain, 1750–1913,” *Explorations in Economic History* 31 (1994), 176–194.
- Cogley, T., and T. J. Sargent, “Measuring Price-level Uncertainty and Instability in the United States, 1850–2012,” *Review of Economics and Statistics* 97 (2015), 827–838.
- Cogley, T., T. J. Sargent and P. Surico, “Price-level Uncertainty and Instability in the United Kingdom,” *Journal of Economic Dynamics & Control* 52 (2015), 1–16.
- Del Negro, M. and G. E. Primiceri, “Time Varying Structural Vector Autoregressions and Monetary Policy: A Corrigendum,” *Review of Economic Studies* 82 (2015), 1342–1345.
- Feinstein, C. H., “A New Look at the Cost of Living,” in J. Foreman-Peck, ed. *New Perspectives on the Late Victorian Economy* (Cambridge, UK: Cambridge University Press, 1991), 151–179.
- Feinstein, C. H., “Pessimism Perpetuated: Real Wages and the Standard of Living in Britain during and after the Industrial Revolution,” *Journal of Economic History* 58 (1998), 625–658.

- Follett, L. and C. Yu, “Achieving Parsimony in Bayesian Vector Autoregressions with the Horseshoe Prior,” *Econometrics and Statistics* 11 (2019), 130–144.
- Harvey, A., E. Ruiz and N. Shephard, “Multivariate Stochastic Variance Models,” *Review of Economic Studies* 61 (1994), 247–264.
- Koop, G., and S. Potter, “Time Varying VARs with Inequality Restrictions,” *Journal of Economic Dynamics & Control* 35 (2011), 1126–1138.
- Lindström, J., “Transformed Proposal Distributions,” mimeo, Centre for Mathematical Sciences, Lund University, 2017 (available at <https://umbertopicchini.files.wordpress.com/2017/12/transformed-proposals2.pdf>).
- Makalic, E. and D. F. Schmidt, “A Simple Sampler for the Horseshoe Estimator,” *IEEE Signal Processing Letters* 23 (2016), 179–182.
- Mitchell, B.R., *British Historical Statistics* (Cambridge, UK: Cambridge University Press, 1988).
- Nason, J. M. and G. W. Smith, “UK Inflation Forecasts since the Thirteenth Century,” CAMA working paper 2021-32, Crawford School of Public Policy, Australian National University, March 2021.
- O’Donoghue J., L. Goulding and G. Allen, “Consumer Price Inflation since 1750,” *Office for National Statistics, Economic Trends* 604 (2004), 38–46.
- Omori, Y., S. Chib, N. Shephard and J. Nakajima, “Stochastic Volatility with Leverage: Fast and Efficient Likelihood Inference,” *Journal of Econometrics* 140 (2007), 425–449.
- Polson, N. G. and J. G. Scott, “On the Half-Cauchy Prior for a Global Scale Parameter,” *Bayesian Analysis* 7 (2012), 887–902.
- Prüser, J., “The Horseshoe Prior for Time-varying Parameter VARs and Monetary Policy,” *Journal of Economic Dynamics & Control* 129 (2021), 104188.
- Thomas, R. and N. Dimsdale, “A Millennium of UK Data,” spreadsheet, Bank of England, 2016 (can be downloaded from <https://www.bankofengland.co.uk/statistics/research-datasets>).
- Vihola, M., “Robust Adaptive Metropolis Algorithm with Coerced Acceptance Rate,” *Statistics and Computing* 22 (2012), 997–1008.